UC Davis

Title

A Conserved Puccinia striiformis Protein Interacts with Wheat NPR1 and Reduces Induction of Pathogenesis-Related Genes in Response to Pathogens.

Permalink

Journal

ISSN

Authors

Wang, Xiaodong
Yang, Baoju
Li, Kun
et al.

Publication Date

DOI

Peer reviewed

1   **A Conserved *Puccinia striiformis* Protein Interacts with Wheat NPR1 and Reduces**

2   **Induction of *Pathogenesis-Related* Genes in Response to Pathogens**

3   Xiaodong Wang [1, 2, 3, #], Baoju Yang [1, #], Kun Li [1, #], Zhensheng Kang [2], Dario Cantu [4], and Jorge

4   Dubcovsky [1, 5]

5

6   [1] Department of Plant Science, University of California, Davis, CA 95616, USA.

7   [2] State Key Laboratory of Crop Stress Biology for Arid Areas and College of Plant Protection,

8   Northwest Agriculture and Forestry University, Yangling, Shaanxi 712100, P. R. China.

9   [3] College of Plant Protection, Biological Control Center for Plant Diseases and Plant Pests of

10   Hebei, Agriculture University of Hebei, Baoding, Hebei 071000, P. R. China.

11   [4] Department of Viticulture and Enology, University of California, Davis, CA 95616, USA.

12   [5] Howard Hughes Medical Institute (HHMI), Chevy Chase, MD 20815, USA.

13

14   Corresponding author: Jorge Dubcovsky, Email: jdubcovsky@ucdavis.edu

15   [#] These authors contributed equally to this work.

1   **ABSTRACT**

2   In Arabidopsis, NPR1 is a key transcriptional co-regulator of systemic acquired

3   resistance. Upon pathogen challenge, NPR1 translocates from the cytoplasm to the

4   nucleus, where it interacts with TGA-bZIP transcription factors to activate the expression

5   of several *Pathogenesis-Related* (*PR*) genes. In a screen of a yeast two-hybrid library

6   from wheat leaves infected with *Puccinia striiformis* f. sp. *tritici*, we identified a

7   conserved rust protein that interacts with wheat NPR1 and named it <u>*Puccinia*</u> <u>NP</u>R1

8   <u>i</u>nteractor (PNPi). PNPi interacts with the NPR1/NIM1-like domain of NPR1 via its

9   C-terminal DPBB_1 domain. Using bimolecular fluorescence complementation assays,

10   we detected the interaction between PNPi and wheat NPR1 in the nucleus of *Nicotiana*

11   *benthamiana* protoplasts. A yeast three-hybrid assay showed that PNPi interaction with

12   NPR1 competes with the interaction between wheat NPR1 and TGA2.2. In barley

13   transgenic lines over expressing *PNPi*, we observed reduced induction of multiple *PR*

14   genes in the region adjacent to *Pseudomonas syringae* pv. *tomato* DC3000 infection.

15   Based on these results, we hypothesize that PNPi has a role in manipulating wheat

16   defense response via its interactions with NPR1.

17

18   **Key words:** wheat; stripe rust; NPR1; pathogen effector; yeast two-hybrid; bimolecular

19   fluorescence complementation; transgenic barley.

20

1 **INTRODUCTION**

2 *Puccinia striiformis* Westend. f. sp. *tritici* Erikss. (*Pst*) is the causal pathogen of wheat

3 stripe rust which is also known as yellow rust. New and more virulent *Pst* races appeared

4 at the beginning of this century and expanded rapidly into many of the wheat growing

5 regions of the world, where they are causing large yield losses (Chen et al., 2002;

6 Hovmøller et al., 2010; Simons et al., 2011; Hovmøller et al., 2016). Many of the

7 resistance genes that were effective against previous *Pst* races became ineffective against

8 these new races (Chen et al., 2002) prompting the search for new sources of resistance

9 (e.g. (Maccaferri et al., 2015)).

10 The successful biotrophic lifestyle of obligate parasitic fungi, such as the rust

11 pathogens, depends upon their ability to deliver specialized effectors into the host cells to

12 suppress or evade plant defenses. Uncovering how these effectors function is critical to

13 understand pathogenicity mechanisms and to develop new strategies to fight these

14 pathogens. Recent whole genome analyses of several *Pst* races revealed a large number

15 of hypothetical effector proteins (Cantu et al., 2011; Cantu et al., 2013b; Zheng et al.,

16 2013). In addition, sixteen *Pst* candidate effectors have been recently characterized in

17 *Nicotiana benthamiana* and their target subcellular compartments have been identified

18 (Petre et al., 2015).

19 Plants are under constant evolutionary pressure to recognize pathogen effectors, or the

20 modifications to their host targets (Jones and Dangl, 2006). This is generally achieved by

3

1 modifications in the recognition sites of intracellular receptors, which frequently belong

2 to the nucleotide-binding leucine-rich receptor (NBS-LRR) class (Michelmore et al.,

3 2013). Once an effector is recognized by the plant, the pathogen is under evolutionary

4 pressure to modify or eliminate this effector to avoid recognition (Raffaele and Kamoun,

5 2012). These recurrent evolutionary processes generate an arms-race between pathogen

6 and host that usually drives a rapid evolution of both resistance genes and effectors.

7   In addition to a local hypersensitive reaction, effector triggered immunity can also

8 result in systemic acquired resistance, an inducible form of plant defense that confers

9 broad-spectrum immunity to secondary infections beyond the initial infection site. In

10 Arabidopsis, this type of resistance involves the generation of mobile signals,

11 accumulation of salicylic acid (SA) hormone, and transcriptional activation of

12 *Pathogenesis-Related* (*PR*) antimicrobial genes (reviewed in (Fu and Dong, 2013)). The

13 Arabidopsis NPR1 protein (NONEXPRESSER OF PR GENES 1, also known as NIM1

14 and SAI1) is a master regulator required for transduction of the SA signal. Upon

15 pathogen infection or artificial SA applications, NPR1 moves from the cytoplasm into the

16 nucleus where it interacts with TGA2 transcription factors to activate multiple *PR* genes

17 (Cao et al., 1994; Delaney et al., 1995; Ryals et al., 1997; Shah et al., 1997; Mou et al.,

18 2003).

19   A previous analysis of the interactions between wheat NPR1 (wNPR1) and wheat

20 homologs of known rice NPR1 interactors confirmed that wNPR1 interacts with four

4

1   members of the basic-region leucine zipper (bZIP) transcription factor family (Cantu et

2   al., 2013a). The interactions between wNPR1 and transcription factors wTGA2.1,

3   wTGA2.2 and wTGA2.3 were also observed between the orthologous proteins in rice

4   (Chern et al., 2001) and Arabidopsis (Després et al., 2003), and are critical to mediate

5   NPR1 function. wLG2, the fourth bZIP transcription factor shown to interact with

6   wNPR1, belongs to a separate subclass, and is similar to the maize protein encoded by

7   the *Liguless* gene (Chern et al., 2001). The wNPR1 protein was also shown to interact

8   with two wheat NRR proteins (Negative Regulator of Resistance) and one NRR paralog

9   designated as wNRRH1 (Cantu et al., 2013a). The rice homologs of the wheat NRR

10   proteins were previously shown to downregulate NPR1 activity (Chern et al., 2005a).

11   NPR1 is a conserved protein that contains three different domains. The BTB/POZ

12   (Broad-complex, Tramtrack, and Bric-a-brac/poxvirus, zinc finger) domain, located at the

13   N-terminal region, is a potential target for ubiquitin-dependent degradation by

14   Cullin3-based E3 ligases (Petroski and Deshaies, 2005). The central ankyrin-repeat

15   domain is predicted to mediate protein-protein interactions with TGAs, and is essential

16   for NPR1 function (Cao et al., 1997; Sedgwick and Smerdon, 1999). The

17   NPR1/NIM1-like domain in the C-terminal region, together with the BTB/POZ domain,

18   is required for SA binding (Wu et al., 2012).

19   In Arabidopsis, NPR1 paralogs NPR3 and NPR4 are involved in the CUL3 E3

20   ligase-mediated degradation of NPR1 in a SA concentration-dependent manner (Fu et al.,

1   2012). At low SA levels, NPR1 is targeted for degradation in proteasomes via its binding

2   to NPR4. As SA level increases after pathogen infection (basal resistance), SA binds to

3   NPR4 releasing more NPR1, which activates the NPR1-mediated plant defense reactions;

4   at very high SA levels (hypersensitive cell death), SA binds to NPR3 and promotes its

5   interaction with NPR1, which finally leads to the turnover of NPR1 (Fu et al., 2012;

6   Moreau et al., 2012).

7   In barley and wheat, the NPR1 resistance mechanism exhibits some differences from

8   the mechanisms described above for Arabidopsis. In wheat, the NPR1-regulated gene

9   *wPR1* was induced by the fungal pathogen *Erysiphe gramini*, but did not respond to SA

10 or its functional analogs 2,6-dichloroisonicotinic acid (INA) and benzothiadiazole (BTH)

11 (Molina et al., 1999). In barley, *HvPR1*, *HvPR3* (chitinase), *HvPR5* (thaumatin-like), and

12 *HvPR9* (peroxidase) showed significant induction after infection with *E. gramini* or

13 *Pseudomonas syringae* pv. *syringae*, but only infection with the latter resulted in higher

14 SA accumulation (Vallelian-Bindschedler et al., 1998). Wheat transgenic lines

15 overexpressing Arabidopsis *NPR1* show a faster activation of defense response to

16 *Fusarium* head blight and expression of *PR1* becomes BTH sensitive (Makandar et al.,

17 2006). Injection of barley leaves with *P. syringae* DC3000, results in acquired resistance

18 in the area adjacent to the pathogen injection, but, in contrast to Arabidopsis, the

19 resistance is not systemic (Colebrook et al., 2012).

20 In this study, we report the identification of a conserved *Pst* protein that interacts with

6

1   wNPR1, and interferes with its binding to transcription factor wTGA2.2. We also show

2   that overexpression of this *Pst* gene in barley results in the reduced induction of *PR* genes

3   in the region adjacent to *P. syringae* infection sites. Based on these results, we

4   hypothesize that this putative effector may have a role in manipulating wheat defense via

5   its protein interaction with wNPR1.

6

7   **RESULTS**

8   ***Pst* PNPi protein interacts with wNPR1 in a yeast two-hybrid (Y2H) screen.**

9   The screening of a Y2H library of *Pst* infected wheat leaves using wNPR1 (JX424315)

10   as bait (primers in Supplementary Table S1) yielded interactions with the wTGA2.2

11   (JX424317) protein (Cantu et al., 2013a) and with a protein from *Pst*, designated here as

12   <u>*Puccinia*</u> <u>N</u>PR1 <u>i</u>nteractor (PNPi, GenBank accession number KT764125). The portion of

13   *PNPi* included in the clone identified in the Y2H screen was 726 bp long and encoded an

14   N-terminal truncated peptide PNPi$_{(93-333)}$ protein. Comparison of the full-length cDNA

15   sequence of PNPi from *Pst* race PST-08/21 (Cantu et al., 2013b) with the genomic

16   sequence of PST-130 (Cantu et al., 2011) showed that the *PNPi* gene has seven exons and

17   encodes a predicted protein of 333 amino acids. The gene structure is annotated in

18   KT764125.

19   The SignalP program predicted the presence of a secretory pathway signal peptide of

1   22 amino acids with high confidence. Twenty-four amino acids after the end of the

2   predicted signal peptide PNPi showed the sequence RSLL-----DEEP, which is similar but

3   not identical to the RxLR-dEER motif frequently found in oomycete effectors.

4   Comparison with the conserved domains in the Pfam database indicated significant

5   similarity of the C-terminal region of PNPi with a "Rare lipoprotein A (RlpA)-like

6   double-psi beta-barrel domain" (DPBB_1 domain, pfam 03330, Fig. 1). No

7   trans-membrane domains were detected using the program TMHMM (Moller et al.,

8   2001).

9   Sequence alignment of PNPi proteins from *Pst* races PST-78 (PSTG_16231,

10   PRJNA123765), PST-21, PST-43, PST-87/7, PST-08/21 and PST-130 (Cantu et al., 2011;

11   Cantu et al., 2013b) and two *Puccinia striiformis* f. sp. *hordei* (*Psh*) races, PSH-54

12   (GenBank accession KT764126) and PSH-72 (GenBank accession KT764127), showed

13   100% identity among all sequences. The coding regions of these genes were also 100%

14   identical at the DNA level.

15   A sequence alignment of the PNPi protein from *Pst* with its homologues from wheat

16   stem rust *Puccinia graminis* f. sp. *tritici* (*Pgt*, XP_003325658) and wheat leaf rust

17   *Puccinia triticina* (*Pt*, PTTG_03809) showed good conservation along the complete

18   protein length (Fig. 1). The PNPi protein from *Pst* is 67.2% similar to the homologous

19   protein in *Pgt* and 66.8% similar to homologous protein in *Pt*. Similarity between PNPi

20   proteins from the wheat rust pathogens and the closest homologs from more distantly

8

1   related plant pathogens (e.g. *Melampsora larici*, *Ustilago maydis*, *Rhizoctonia solani*, etc.)

2   were limited to the C-terminal region including the DPBB_1 domain (Supplementary Fig.

3   S1). Only this conserved region was used to generate the phylogenetic tree presented in

4   Supplementary Fig. S2.

5

6   ***PNPi* is up-regulated during the late stages of *Pst* infection.**

7   After inoculation of the susceptible common wheat variety "Fielder" with the virulent

8   *Pst* race PST-130, we collected leaves at 5, 8, 15 and 22 days post inoculation (dpi). The

9   first two collection points were done during haustoria formation and secondary hyphae

10   expansion, whereas samples for the 15 dpi and 22 dpi were collected during the initiation

11   and full development of the sporulation phase, respectively.

12   Analysis of *PNPi* expression at the four time points using qRT-PCR (primers in

13   Supplementary Table S2) showed a clear up-regulation from 8 to 22 dpi (Supplementary

14   Fig. S3). Analysis of published transcriptome data showed that *PNPi* is expressed in two

15   datasets from isolated *Pst* haustoria (Cantu et al., 2013b; Garnica et al., 2013), but not in

16   the dataset from germinated urediniospores (Garnica et al., 2013). *PNPi* expression was

17   detected in RNA extracted from haustoria (Cantu et al., 2013b) at 9 dpi (Garnica et al.,

18   2013) and from a pool of haustoria collected at 6 and 14 dpi (Cantu et al., 2013b). These

19   data suggest that *PNPi* is expressed in the mature haustoria.

1

2 **The DPBB_1 domain in PNPi interacts with the NPR1/NIM1-like domain in**

3 **wNPR1.**

4   The full length wNPR1 (JX424315) and a truncated PNPi$_{(23-333)}$ protein lacking the

5 signal peptide (to avoid secretion) showed a strong interaction in the Y2H assays under

6 SD selection media lacking both Histidine and Adenine (SD-Leu-Trp-His-Ade) (Fig. 2B,

7 and negative controls for Y2H assays in Supplementary Fig. S4). To determine which

8 portion of the PNPi and wNPR1 proteins were responsible for their interaction, we tested

9 two fragments of PNPi and three fragments of wNPR1 by Y2H assays (Fig. 2A). The

10 N-terminal region of PNPi$_{(23-235)}$ failed to interact with the complete wNPR1. By contrast,

11 the C-terminal region of PNPi$_{(236-333)}$ including the DPBB_1 domain showed a strong

12 interaction with wNPR1 in SD-Leu-Trp-His-Ade selection medium (Fig. 2B).

13   We then tested the interactions between the PNPi$_{(23-333)}$ protein lacking the signal

14 peptide with each of the three wNPR1 fragments. Both the N-terminal wNPR1$_{(1-170)}$ and

15 the central part wNPR1$_{(196-363)}$ including the DUF3420 and ANK domain showed no

16 interaction with PNPi$_{(23-333)}$. By contrast, the C-terminal wNPR1$_{(355-572)}$ region including

17 the NPR1/NIM1-like domain interacted with PNPi$_{(236-333)}$ in SD-Leu-Trp-His-Ade

18 selection medium (Fig. 2B). Similar results were observed when PNPi$_{(23-333)}$ was replaced

19 by the C-terminal region PNPi$_{(236-333)}$ (Fig. 2B). PNPi$_{(23-333)}$ also interacted in Y2H assays

20 with the NPR1 homolog from Arabidopsis, suggesting that PNPi recognizes a conserved

10

1   region in NPR1 (Fig. 2B).

2   We then tested the ability of PNPi$_{(23\text{-}333)}$ to interact with the NPR1/NIM1-like domain

3   from wNPR1 paralogs wNPR3 (Td-k36_contig_20687) and wNPR4 (Td-k56_contig_528)

4   from tetraploid wheat Kronos (Krasileva et al., 2013). A strong interaction was detected

5   between PNPi$_{(23\text{-}333)}$ and wNPR4$_{(385\text{-}607)}$ in SD-Leu-Trp-His-Ade selection media, but no

6   interaction was observed for wNPR3$_{(377\text{-}593)}$ (Fig. 2B). For all the negative Y2H assays,

7   we confirmed by Western blots that the proteins were expressed (Supplementary Fig. S5).

8   We then generated amino acid substitution mutations at the conserved sites of DPBB_1

9   domain in PNPi based on the multi-sequences alignment (Supplementary Fig. S1). The

10   point mutation C301W in PNPi$_{(23\text{-}333)}$ was sufficient to abolish the protein interaction

11   between PNPi$_{(23\text{-}333)}$ and wNPR1 in all three dilutions (in SD-Leu-Trp-His-Ade selection

12   media). Point mutations at the other 14 conserved sites of the DPBB_1 domain showed

13   interactions in all three dilutions in SD-Leu-Trp-His-Ade, with the exception of D257W

14   that was not detected only in the 1:1 and 1:10 dilutions (Supplementary Fig. S6).

15

16   **PNPi-wNPR1 interaction was validated in *N. benthamiana* protoplasts.**

17   To validate the Y2H interaction between wNPR1 and PNPi, we performed bimolecular

18   fluorescence complementation (BiFC) assays. Co-expression of YFP^{N}-PNPi$_{(23\text{-}333)}$ and

19   YFP^{C}-wNPR1 in *N. benthamiana* protoplast resulted in strong YFP fluorescence in the

1   nucleus. We also observed clear YFP fluorescence in the positive control

2   YFP^N-wHSP90.3 (ADF31760.1) / YFP^C-wRAR1 (EF202841.1), and no fluorescence in

3   the negative controls using empty vector constructs YFP^N-EV and YFP^C-EV (Fig. 3). As

4   an additional negative control, we used the nuclear localized protein wFDL2 (EU307112),

5   which interacts with wFT1 (Li et al., 2015) but not with PNPi or NPR1. Protoplast

6   co-transformed with YFP^N-wFDL2 and YFP^C-wFT1 showed strong YFP signal in the

7   nucleus, whereas no fluorescence was detected in protoplasts co-transformed with

8   YFP^N-PNPi$_{(23-333)}$ / YFP^C-wFDL2 or YFP^N-wFDL2 / YFP^C-wNPR1 (Supplementary Fig.

9   S7). For the negative BiFC assays, we confirmed by Western blots that the proteins were

10   expressed in the transformed *N. benthamiana* protoplast (Supplementary Fig. S8).

11

12   **PNPi competes with wTGA2.2 binding to wNPR1 in yeast three-hybrid (Y3H)**

13   **assays.**

14   A Y3H experiment based on the pBridge vector was performed to test if PNPi

15   interferes with the interaction between wNPR1 and wTGA2.2 (Cantu et al., 2013a). The

16   pBridge vector allows the expression of two proteins: a DNA-binding (BD) fusion, and a

17   second protein that positively or negatively affects the interaction between the BD and

18   activation domain (AD) fusion, which is expressed in a separate vector. The second

19   protein (designated Bridge protein) is conditionally expressed under the *MET*25

20   (henceforth M25) promoter only in the absence of methionine (Met), and is repressed in

12

1   its presence.

2   Two different reporters, Aureobasidin A (Aba) and X-α-Gal, were included in the Y3H

3   assays to visualize the strength of the protein-protein interactions. Expression of the

4   *AUR1-C* dominant mutant in response to protein-protein interactions in the Y2HGold

5   yeast strain confers strong resistance to the otherwise highly toxic Aba drug (Clontech,

6   2013). The left panels of Fig. 4A excluding Aba selection are used as transformation

7   controls (only transformants containing both bait and prey vectors can grow on

8   SD-Leu-Trp) and to confirm the correct normalization of the loaded samples to similar

9   numbers of yeast cells. In the presence of Aba, a clear reduction in the strength of the

10   wNPR1 and wTGA2.2 interaction was detected in the presence of $PNPi_{(23-333)}$ (-Met)

11   compared with the absence of $PNPi_{(23-333)}$ (+Met) (Fig. 4A, indicated by arrows). This

12   result suggests that $PNPi_{(23-333)}$ interferes with the wNPR1-wTGA2.2 interaction. This

13   competitive effect of PNPi can be also observed by comparing the construct expressing

14   both the $PNPi_{(23-333)}$ and wTGA2.2-BD protein with the construct including only the

15   wTGA2.2-BD protein (both in -Met, Fig. 4A). This effect was also observed in X-α-Gal

16   reporter assays. The blue color of the reporter is less intense in the presence of $PNPi_{(23-333)}$

17   than in its absence (Fig. 4B). The $PNPi_{(23-333)}$-BD construct is included in both assays as a

18   positive control of the interaction between $PNPi_{(23-333)}$ and wNPR1.

19   To quantify the extent of the interference of $PNPi_{(23-333)}$ on the wTGA2.2-wNPR1

20   interaction, we performed a quantitative α- galactosidase assay. In this assay, the α-

13

1   galactosidase activity generated by the interaction between wTGA2.2 and wNPR1 was 40%

2   lower ($P < 0.01$), in the presence of PNPi$_{(23-333)}$ (-Met) than in its absence (+Met) (Fig.

3   4C). Since we found no interaction between PNPi$_{(23-333)}$ and wTGA2.2 by Y2H (Fig. 2B

4   and Supplementary Fig. S4), these results support the hypothesis that PNPi competes

5   with wTGA2.2 for interaction with wNPR1 protein.

6

7   **PNPi signal peptide was sufficient to induce invertase secretion**

8   A yeast invertase secretion assay (Gu et al., 2011) was used for the functional

9   validation of PNPi predicted signal peptide (22 amino acids). Yeast YTK12 strain

10   transformed with the pSUC2 vector including the signal peptide of PNPi fused in frame

11   to the invertase sequence were able to grow in both the SD-Trp and YPRAA medium

12   (Supplementary Fig. S9). By contrast, the YTK12 control strain that is unable to secrete

13   invertase could not grow on the YPRAA medium (Supplementary Fig. S9 includes

14   additional negative Mg87$_{(1-25)}$-pSUC2 and positive Ps87$_{(1-25)}$-pSUC2 controls).

15   Attempts to test re-entry of PNPi into the plant cells using Agro-mediated

16   transformation of *N. benthamiana* were not successful. We were unable to detect

17   secretion of the predicted signal peptide (PNPi$_{(1-22)}$) fused with GFP in *N. benthamiana*

18   plasmolyzed epidermal cells (Supplementary Fig. S10). PNPi$_{(1-22)}$-GFP fusion showed a

19   similar cytoplasmic localization as the fusions including a larger N-terminal region

20   (PNPi$_{(1-64)}$-GFP), the complete PNPi protein (PNPi$_{(1-333)}$-GFP) or the GFP control

14

1   (Supplementary Fig. S10).

2

3   **Overexpression of *PNPi* reduces induction of *pathogenesis-related* (*PR*) genes.**

4   Based on the previous experiment, we hypothesized that the interference of PNPi on

5   the wTGA2.2-wNPR1 interaction could also interfere with the wNPR1 regulation of

6   downstream *PR* genes. To test this hypothesis we generated transgenic barley plants

7   overexpressing *PNPi*(23-333) (without the signal peptide) under the maize *Ubiquitin*

8   promoter. Four independent transgenic events were obtained and confirmed both by PCR

9   of genomic DNA and qRT-PCR. Expression levels of the *PNPi* transgene were between 4

10   and 17% of the levels of *HvEF1a* endogenous control (Supplementary Fig. S11).

11   *PR* genes were induced in the leaves of both transgenic and control untransformed

12   plants by inoculation with *P. syringae* pv. *tomato* DC3000 infection (Fig. 5A) as

13   described before in similar experiments performed with the same barley variety used here

14   (Colebrook et al., 2012). All five *PR* genes showed induction in the adjacent region to the

15   *P. syringae* inoculation (48 h after inoculation) relative to the regions adjacent to the

16   water infiltrated control. We present the results for transgenic Event_1 in Fig. 5B-F and

17   those for events 2, 3, and 4 in Supplementary Fig. S12. The *P* values presented below Fig.

18   5B-F panels indicate the significance of the differences between *PNPi* transgenic plants

19   and their isogenic controls in combined ANOVAs using the four transgenic events as

20   blocks. Comparison of the regions adjacent to the *Pseudomonas* inoculation showed

15

1   significant differences between the transgenic plants and the non-transgenic control for

2   *HvPR1b* (P = 0.006, Fig. 5B), *HvPR2* (P = 0.001, Fig. 5C), *HvPR4b* (P = 0.018, Fig. 5D),

3   *HvPR5* (P = 0.032, Fig. 5E), and *HvChitinase 2a* (P = 0.004, Fig. 5F). The differences

4   were consistent in all four transgenic events for all five genes: expression levels were

5   lower in the transgenic plants overexpressing *PNPi* than in the non-transgenic control. By

6   contrast, none of the five *PR* genes showed significant differences between transgenic

7   and control plants in water-inoculated control plants (Fig. 5 and Supplementary Fig. S12).

8   This experiment cannot be done using *Psh* instead of *P. syringae* because the rust

9   pathogen would introduce to the control plants the same PNPi protein expressed in the

10   transgenic barley plants.

11   Previous studies in Arabidopsis have shown that NPR1 interactions with TGA

12   transcription factors play an important role in the regulation of several *PR* genes (Després

13   et al., 2000; Kinkema et al., 2000). Therefore, we hypothesized that the observed

14   downregulation of the *PR* genes in the PNPi transgenic plants could be associated with

15   the ability of PNPi to interfere with the NPR1 and TGA protein interactions (Fig. 4). To

16   test the connection between NPR1 and the *PR* genes in Triticeae species, we

17   overexpressed the wheat *NPR1* gene under the maize *Ubiquitin* promoter (*Ubi::wNPR1*)

18   in barley and obtained two independent transgenic events with 1.8- and 6.3-fold higher

19   *NPR1* transcript levels than the wild type (Supplementary Fig. S13). We also obtained

20   previously published RNA interference (RNAi) barley transgenic plants with reduced

16

1   transcript levels of *HvNPR1* (32% and 46% of the wild type levels, Supplementary Fig.

2   S13) (Dey et al., 2014).

3   After inoculation with *P. syringae* pv. *tomato* DC3000 we extracted RNA from the

4   region adjacent to the infection area and evaluated *PR* genes expression. In the RNAi

5   transgenic plants with knocked-down *HvNPR1* transcript levels, we observed a decrease

6   in the relative expression of several barley *PR* genes, which was significant for *HvPR1b*,

7   *HvPR4b*, and *HvChitinase 2a* (Supplementary Fig. S14). In the transgenic barley plants

8   overexpressing *wNPR1* (*Ubi::wNPR1*), we observed a significant increase in the

9   transcript levels of all tested *PR* genes relative to the control (Supplementary Fig. S15).

10   The overexpression of the *NPR1* gene was stronger in the transgenic event 7 than in event

11   8 and this was correlated with a stronger induction of the *PR* genes in transgenic event 7

12   (Supplementary Fig. S13). In the control plants inoculated with water, we detected no

13   significant differences, except for *PR1b* in the *Ubi::wNPR1* transgenic plants

14   (Supplementary Fig. S14 and S15).

15

16   **DISCUSSION**

17   **Discovery of a putative *Pst* effector that directly targets wNPR1.**

18   The Y2H system has been used for both the discovery and validation of protein

19   interaction between pathogen effectors and plant defense-related proteins. Good

1   examples of this strategy include the interactions between the CSEP0055 effector from

2   *Blumeria graminis* f. sp. *hordei* and barley defense protein PR17c (Zhang et al., 2012),

3   between the *Parastagonospora nodorum* effector SnTox3 and wheat TaPR1 (Breen et al.,

4   2016), and between the AvrL567 effector from *Melampsora lini* and L5/L6 R protein

5   from flax (Ravensdale et al., 2012). In this study, we screened a Y2H library from *Pst*

6   infected wheat leaves to identify *Pst* proteins that interact with wNPR1, a master

7   regulator of systemic acquired resistance.

8   The conservation of NPR1 protein interactions between wheat and rice (Cantu et al.,

9   2013a), and between rice and Arabidopsis (Després et al., 2003; Chern et al., 2005b),

10   suggests that this is an ancient component of the plant immune system. The conservation

11   of NPR1 protein sequence across the monocot-dicot divide (Supplementary Fig. S16) is

12   also supported in this study by the ability of both wheat and Arabidopsis NPR1 proteins

13   to interact with PNPi (Fig. 2B). The discovery of this interaction was an exciting result,

14   because no pathogen effector has been reported so far to target NPR1 directly. There are,

15   however, multiple effectors from different pathogens that have been reported to target

16   NPR1 indirectly by targeting SA-mediated plant defense pathway (reviewed in (Kazan

17   and Lyons, 2014)). For example, the type III effector XopJ from *Xanthomonas*

18   *campestris* interacts with the plant proteasomal subunit RPT6 and is involved in the

19   reduction of salicylic acid (Üstün et al., 2013). Two additional examples are the downy

20   mildew effector HaRxL44, which interacts with Mediator subunit 19a in a

1. proteasome-dependent manner, suppressing SA-triggered immunity in Arabidopsis

2. (Caillaud et al., 2013); and the *Cmu1* effector from *Ustilago maydis*, which affects both

3. pathogen virulence and SA levels in the *Z. mays* host plant (Djamei et al., 2011). Finally,

4. the HopM1 effector from *P. syringae* pv. *tomato* DC3000 suppresses expression of *PR1*

5. by targeting AtMIN7 (Gangadharan et al., 2013).

6.   The direct PNPi-wNPR1 interaction detected in the Y2H screen was validated by

7. bimolecular fluorescence complementation in *N. benthamiana* protoplasts (Fig. 3), and

8. was characterized in more detail by testing interactions between different regions of both

9. proteins and different PNPi mutants by Y2H. Strong interactions were observed between

10. DPBB_1 and NPR1/NIM1-like domains, located in the C-terminal regions of PNPi and

11. wNPR1, respectively. We also showed that the amino acid substitution C301W in the

12. DPBB_1 domain of PNPi is sufficient to abolish its interaction with NPR1

13. (Supplementary Fig. S6). The DPBB_1 domain of PNPi was also shown to interact in the

14. Y2H assays with the C-terminal region of the wNPR1 homolog wNPR4, which encodes a

15. proteasomal adaptor protein that regulates proteasome-mediated turnover of NPR1 in a

16. SA-dependent manner (Fu et al., 2012). These results suggest that PNPi may affect both

17. the function of wNPR1 on disease resistance and/or affect its stability through its

18. interactions with wNPR4.

19.

20. **Characterization of the PNPi putative effector.**

1   Several lines of evidence suggest that the protein encoded by *PNPi* is an effector. This

2   is a small protein (333 amino acids) with a secretory signal peptide that is encoded by a

3   gene expressed in the haustoria. In addition, it interacts with at least two host proteins

4   (wNPR1 and wNPR4), and when over expressed in barley cells it downregulates the

5   induction of *PR* genes after pathogen infection. However, the evolutionary conservation

6   of the PNPi protein sequence among a relatively wide range of plant pathogens is an

7   unusual characteristic for an effector. The continuous arms race between resistance genes

8   and effectors, usually results in a rapid evolution of both gene classes. Signatures of

9   positive selection are often found when comparing strain-specific variants of protein

10   effectors suggesting that effectors play a key role in the arms race with the host immune

11   system (Guttman et al., 2014). By contrast, PNPi seems to be conserved, not only among

12   different *Pst* races but also among different *formae specialis*. Not a single amino acid

13   change was observed between the different *Pst* and *Psh* races sequenced in this study. A

14   relatively high level of conservation was also observed among PNPi proteins from wheat

15   stripe, leaf and stem rust pathogens (Fig. 1). These results suggest that PNPi likely plays

16   an important role in the evolutionary success of this group of pathogens and that changes

17   in the structure of this protein are under evolutionary constrains.

18

19   **Secretion and localization of PNPi.**

20   To interact with its target protein NPR1, PNPi needs to be secreted first from the *Pst*

1   cells into the extra-haustorial matrix, and then translocated into the host cells. The

2   predicted signal peptide of PNPi was sufficient to induce invertase secretion from

3   transformed yeast cells (Supplementary Fig. S9). However, we were unable to detect

4   secretion of the predicted signal peptide (PNPi$_{(1-22)}$) fused with GFP in *N. benthamiana*

5   plasmolyzed epidermal cells (Supplementary Fig. S10).

6   The RSLL-----DEEP sequence in the N-terminal region of PNPi is similar but not

7   identical to the RxLR-dEER amino acid motif observed in many oomycete effectors

8   (Kale and Tyler, 2011; Wang et al., 2011). In *Phytophthora sojae* effectors, the

9   RxLR-dEER motif has been proposed to be sufficient for re-entry into plant cells, even in

10   the absence of the pathogen (Dou et al., 2008; Wang et al., 2011). However, a recent

11   study in *N. benthamiana* failed to show re-entry into plant cells of effectors from

12   *Melampsora lini* and *Phytophthora infestans* fused to a signal peptide and fluorescent

13   proteins (Petre et al., 2016). Therefore, other methods may be required to test the role of

14   PNPi RSLL-----DEEP region in plant cell entry.

15

16   **Effect of PNPi on the induction of *pathogenesis-related* genes and the potential role**

17   **of wNPR1**

18   In Arabidopsis, pathogen infection or SA treatment results in the translocation of NPR1

19   from the cytoplasm to the nucleus, its interaction with TGA transcription factors, the

20   up-regulation of a large set of *PR* genes, and the establishment of systemic acquired

21

1   resistance (Zhang et al., 1999; Després et al., 2000; Kinkema et al., 2000; Fan and Dong,

2   2002). In rice, which has higher endogenous levels of SA, *PR* genes are not effectively

3   induced at SA concentrations that are effective in dicot species. However, at high SA

4   concentrations some *PR* gene induction is observed (Ganesan and Thomas, 2001). In

5   spite of the limited effect of SA on the activation of *PR* genes in rice, transgenic

6   over-expression of *NPR1* in this species results in constitutive activation of defense

7   responses and improved resistance to bacterial blight (Chern et al., 2005b; Yuan et al.,

8   2007). We also observed in this study a higher level of *PR* induction by *P. syringae* in

9   barley plants overexpressing the wheat *NPR1* gene (Supplementary Fig. S15). In addition,

10 down-regulation of *NPR1* in rice leads to loss of resistance to the rice blast fungus

11 *Magnaporthe grisea* (Sugano et al., 2010; Feng et al., 2011) and in barley to enhanced

12 susceptibility to *Blumeria graminis* f. sp. *hordei*, (Dey et al., 2014). This is consistent

13 with the reduced induction of several barley *PR* genes by *P. syringae* in the transgenic

14 RNAi plants with reduced expression of *HvNPR1* (Supplementary Fig. S14). These

15 results suggest that monocot and dicot plants share some parts of the signal transduction

16 pathway controlling NPR1-mediated resistance (Chern et al., 2001). When wheat and

17 barley plants are exposed to various pathogens, *PR* genes show a very similar induction

18 as in Arabidopsis and rice (Colebrook et al., 2012; Dey et al., 2014). However, wheat and

19 barley *PR* genes are not induced by SA or BTH treatment as in the previous two model

20 species (Kogel et al., 1994; Vallelian-Bindschedler et al., 1998; Colebrook et al., 2012).

22

1   This suggests that the enhanced resistance observed in wheat and barley leaves treated

2   with BTH, is likely dependent on the up-regulation of a different set of resistance genes

3   (Görlach et al., 1996; Besser et al., 2000).

4   In barley and wheat, the induction of *PR* genes in the region adjacent to the infiltration

5   with *P. syringae* pv. *tomato* DC3000 does not expand beyond the infected leaf (Colebrook

6   et al., 2012). This indicates that the response is not systemic as in Arabidopsis and

7   therefore, should be referred as "acquired resistance" rather than as "systemic acquired

8   resistance". A recent research reported that the acquired resistance observed after

9   infection of barley leaves with *P. syringae* pv. *japonica* is associated with a moderate

10   local but not systemic induction of abscisic acid (Dey et al., 2014). The significant

11   induction of five different barley *PR* genes (including *HvPR1b*, *HvPR2*, *HvPR4b*, *HvPR5*,

12   and *HvChitinase 2a*) in the leaf region adjacent to a *P. syringae* infiltration was not

13   observed in plants infiltrated with water, demonstrating a specific response to the

14   pathogen.

15   In this study, we show that the induction of these five *PR* genes by *P. syringae* is

16   significantly reduced in barley plants overexpressing *PNPi* (Fig. 5 and Supplementary

17   Fig. S12), and hypothesize that NPR1 is involved in this reduction. This hypothesis is

18   based on the connection observed between NPR1 and *PR* genes in barley plants with up-

19   or down-regulated levels of *NPR1* (Supplementary Fig. S15 and S14) and on the reduced

20   interactions between wNPR1 and wTGA2.2 proteins observed in the presence of PNPi in

1   Y3H assays (Fig. 4). Previous studies in rice and Arabidopsis have demonstrated that the

2   interactions between NPR1 and different TGA2 transcription factors are critical to

3   mediate the upregulation of multiple *PR* genes (Chern et al., 2001; Després et al., 2003;

4   Johnson et al., 2003). Therefore, the PNPi disruption of this interaction provides a simple

5   hypothesis to explain the reduced induction of *PR* genes observed in the barley plants

6   overexpressing *PNPi*. This reduction also suggests that PNPi plays a role in the

7   manipulation of the wheat defense response, and that it may contribute to the virulence of

8   the rust pathogens. We are currently developing a null *NPR1* mutant in tetraploid wheat

9   to test its effect on *Pst* resistance.

10

11   **MATERIALS AND METHODS**

12   **Screening of Y2H library using wheat wNPR1 as bait.**

13   A yeast two-hybrid (Y2H) cDNA library was previously developed from *Pst* infected

14   and non-infected leaves of *T. turgidum* ssp. *durum* cv. Langdon (Yang et al., 2013).

15   Briefly, RNAs were reverse transcribed into cDNA using the "Make Your Own Mate &

16   Plate Library System" following the company's protocol (Clontech, Mountain View, CA,

17   USA). The cDNA was then recombined into the library prey vector (pGADT7Rec) using

18   Clontech's SMART technology. The final library was transformed into the yeast strain

19   Y187 (MATα) following the Clontech protocol.

1   The cDNA library was screened using the full-length w*NPR1* sequence as bait. w*NPR1*

2   was cloned into the Y2H bait vectors pLAW10 (Cantu et al., 2013a) and introduced into

3   the yeast strain "Y2H Gold" (Clontech, Mountain View, CA, USA) using the lithium

4   acetate method (Gietz and Woods, 2002; Cantu et al., 2013a). wNPR1 does not show

5   auto-activation when tested against an empty vector on SD-Leu-Trp-His-Ade (Cantu et

6   al., 2013a). The bait colonies of pLAW10-wNPR1 were grown to approximately 10^8

7   cfu/ml in 50 ml liquid medium of SD-Trp. Yeast cells were pelleted, washed once with

8   sterile H_2O and resuspended in 50 ml liquid media of 2×YPAD. One aliquot of the Y187

9   target yeast (>2×10^7cells) was combined with the bait. Yeast strains were allowed to mate

10   for 20-24 hours at 30°C with slight shaking. Yeast cells were then isolated and washed

11   twice with sterile water and plated on SD media lacking Leucine, Tryptophan, Histidine

12   and Adenine (SD-Leu-Trp-His-Ade). Yeast putative positive diploids from the primary

13   screens were isolated and plasmids extracted using Zymoprep I™ Yeast Plasmid

14   Minipreparation Kit (Zymo Research,CA,USA). The Matchmaker AD-LD primers were

15   used to amplify the inserted gene fragments (Supplementary Table S1). Sequence

16   annotation were carried out with Blastx homology searches against the NCBI GenBank

17   nr database.

18

19   **Cloning and characterization of *PNPi*.**

20   The primers designed to amplify the coding region of the wNPR1 interactor PNPi

1   identified in the Y2H screen are described in Supplementary Table S1. The complete

2   coding region of *PNPi* was amplified from cDNA synthesized using the RNA isolated

3   from seedling leaves of *Triticum turgidum* ssp. *durum* cv. Langdon line RSL65 infected

4   with *Puccinia striiformis* f. sp. *tritici* race PST-113 and harvested at 24 hours

5   post-inoculation.

6   The predicted amino acid sequence of PNPi protein was used to search the Pfam

7   database (Finn et al., 2014) to identify conserved domains or motifs. SignalP v 4.0 was

8   used to identify signal peptides (Petersen et al., 2011) and TMHMM v2 to detect the

9   presence of trans-membrane domains (Moller et al., 2001). Multiple sequence alignments

10   and Neighbor Joining trees were genrerated using MUSCLE as implemented in MEGA6

11   (Tamura et al., 2013). Confidence of nodes in the Neighbor Joining trees were calculated

12   using 1,000 bootstrap cycles.

13

14   **Expression profile of *PNPi* by qRT-PCR assay.**

15   Seedlings of the susceptible common wheat cultivar Fielder were inoculated with *P.*

16   *striiformis* f. sp. *tritici* race PST-130 (virulent) in a CONVIRON growth chamber as

17   described before (Cantu et al., 2013b). Leaves were harvested at 0, 5, 8, 15 and 22 days

18   post-inoculation (dpi) for RNA isolation. Sporulation was observed at 15 dpi. All samples

19   were rapidly frozen in liquid nitrogen and stored at -80°C. Four independent biological

20   replications were included for each time point.

1   The mRNAs were isolated using the MagMAX™ express magnetic particle processors

2   (Thermo Fisher Scientific) according to the manufacturer's instructions. First-strand

3   cDNA was synthesized using the Reverse Transcription kit (Applied Biosystem).

4   Quantitative reverse transcription PCR (qRT-PCR) was performed using SYBR Green[®]

5   (Life Technologies) and a 7500 Fast Real-Time PCR system (Applied Biosystems). Stripe

6   rust elongation factor (*PstEF*, Supplementary Table S2) was used as internal reference.

7   Transcript levels were expressed as linearized fold-*PstEF* levels calculated by the

8   formula $2^{(PstEF\,C_T - TARGET\,C_T)}$. Primer sequences and amplification efficiencies are listed in

9   Supplementary Table S2. Dissociation curves were generated for each primer to confirm

10   primer specificity.

11

12   **Dissection of protein regions involved in PNPi and wNPR1 Y2H interactions.**

13   Different regions of the *PNPi* and *wNPR1* genes were cloned into Y2H vectors

14   pLAW10 (DNA-binding domain, BD) and pLAW11 (activation domain, AD). These

15   vectors were provided by Richard Michelmore (University of California, Davis) and were

16   described before (Cantu et al., 2013a). Two non-overlapping regions of *PNPi* were cloned

17   into pLAW10. The first one included PNPi$_{(23-235)}$, which started immediately after the end

18   of the 22- amino acid long predicted signal peptide and included 213 amino acids from

19   the N-terminal region of the PNPi protein. The second one, designated as PNPi$_{(236-333)}$,

20   included the DPBB_1 domain located in the C-terminal region of the protein.

27

1 Three regions of *wNPR1* were cloned into the pLAW11 vector. Clone wNPR1$_{(1-170)}$,

2 included the BTB/POZ domain, clone wNPR1$_{(196-363)}$ the DUF3420 and ANK domains

3 and clone wNPR1 $_{(355-572)}$ the NPR1/NIM1-like domain. This last domain was also cloned

4 into the bait vector from wNPR1 paralogs wNPR3 (wNPR3$_{(373-593)}$) and wNPR4

5 (wNPR4$_{(385-607)}$). A bait vector with the full-length Arabidopsis *NPR1* homolog and a prey

6 vector with a full length *wTGA2.2* gene were obtained from a previous study (Cantu et al.,

7 2013a). We generated also fifteen amino acid substitutions at conserved sites of the

8 DPBB_1 domain in PNPi by overlap-PCR, and incorporated them into Y2H BD vectors

9 (primers in Supplementary Table 1). The co-transformed yeast strains were assayed on

10 plates with SD-Leu-Trp-His and SD-Leu-Trp-His-Ade selection media.

11   For Y2H assays showing negative results, we confirmed the presence of the proteins

12 using Western blots. Transformed yeast strains were shaken in SD medium overnight, and

13 1 ml of the overnight culture was transferred into fresh YPDA medium until they reached

14 a 0.1 optical density at 600 nm (OD$_{600}$). Samples were then incubated at 30 °C for ~5h

15 with shaking at 230 nm until they reached an OD$_{600}$= 0.4 to 0.6. Yeast cells were

16 harvested by centrifugation. The pellet was washed with ice-cold water, was resuspended

17 in 100 µl of water, and was incubated for 10 min at room temperature with additional 100

18 µl 0.2M NaOH. After a brief centrifugation at 13,000 rpm briefly, the supernatant was

19 removed and 50 µl of SDS-PAGE buffer was added. From each sample, 50 µl was loaded

20 in an SDS-PAGE gel. Protein expression in cells transformed with the Y2H AD vector

1   was detected using the anti-HA-HRP antibody (1:2000 dilution, Sigma

2   Catalog#12013819001), and in those transformed with Y2H BD using the

3   anti-cMyc-HRP antibody (1:500 dilution, Santa Cruz Biotechnology Catalog#9E10).

4

5   **Validation of PNPi-wNPR1 interactions using bimolecular fluorescence**

6   **complementation.**

7   Bimolecular fluorescence complementation (BiFC) assays were conducted using a split

8   yellow fluorescent protein (YFP) system (Bracha-Drori et al., 2004) in *N. benthamiana*

9   protoplasts as described before (Schütze et al., 2009; Cantu et al., 2013a; Wang et al.,

10   2014). The complete coding region of *wNPR1* and of a truncated PNPi excluding the

11   signal peptide were recombined with the N-terminal and C-terminal regions of YFP in

12   Gateway destination vectors pSY736 (YFP^N-PNPi$_{(23-333)}$ fusion) and pSY735

13   (YFP^C-wNPR1 fusion), respectively. The fusion proteins were co-expressed in *N.*

14   *benthamiana* protoplasts using the polyethylene glycol method. Fluorescence was

15   monitored between 24 and 48 h after transformation using a Zeiss Axiovert 25

16   fluorescence microscope with the Zeiss YFP filter cube 46HE (excitation, BP500/25;

17   beam splitter, FT515; emission, BP535/30).

18   Co-transformation of wHSP90.3-pSY736 and wRAR1-pSY735 vectors was used as

19   positive control and co-transformations of YFP^N-PNPi$_{(23-333)}$ and YFP^C-wNPR1 with

20   empty vectors YFP^C-EV and YFP^N-EV, respectively, were used as negative controls. As

29

1   an additional control for false positive nucleic signals, we used the nuclear wheat protein

2   wFDL2 from previous research (Li et al., 2015). Co-transformation of wFDL2-pSY736

3   and wFT1-pSY735 vectors was used to confirm the previously published interaction (Li

4   et al., 2015), whereas co-transformations of YFP^N-PNPi$_{(23-333)}$ and YFP^C-wNPR1 with

5   YFP^C-wFDL2 and YFP^N-wFDL2, respectively, were used as negative controls.

6   In the BiFC assays showing negative results, we confirmed protein expression by

7   Western blots. Transformed protoplasts were collected by centrifugation at 100 g for 4

8   min. After removing half of the supernatant, we added 50 µl of SDS-PAGE sample buffer,

9   boiled the samples for 10 min, centrifuged them at 12000 rpm for 10 min, and loaded 50

10   µl in the SDS-PAGE gel. To detect protein expression, we used anti-HA-HRP antibodies

11   (1:2000 dilution, Sigma Catalog#12013819001) for the protoplasts transformed with the

12   BiFC pSY736 vector, and anti-cMyc-HRP antibodies (1:500 dilution, Santa Cruz

13   Biotechnology Catalog#9E10) for the protoplasts transformed with the BiFC pSY735

14   vector.

15

16   **Subcellular localization.**

17   To study the function of PNPi signal peptide and N-terminal region on subcellular

18   localization, we generated four constructs using GFP fusions in vector pGWB5.

19   Construct 35S::PNPi$_{(1-22)}$-GFP included only the signal peptide of PNPi fused to GFP.

20   Construct 35S::PNPi$_{(1-64)}$-GFP included both the signal peptide and the N-terminal region

30

1   of PNPi fused to GFP. Finally, constructs 35S::PNPi$_{(1-333)}$-GFP included the complete

2   PNPi coding region. These constructs were transformed into *Agrobacterium* strain

3   GV3101 (Hofgen and Willmitzer, 1988). Infiltration experiments were performed on

4   four- to six-week-old *N. benthamiana* plants as described before (Wang et al., 2011). An

5   empty pGWB5 vector expressing only GFP was used as control. Green fluorescence was

6   detected 48 h after infiltration by fluorescence microscopy. Epidermal peels from *N.*

7   *benthamiana* leaves were plasmolyzed in 800 mM mannitol for six minutes.

8

9   **Yeast secretion assays for the validation of signal peptide of PNPi.**

10   The signal peptide of PNPi$_{(1-22)}$ was fused in frame to the invertase sequence in the

11   pSUC2 vector and were transformed into yeast strain YTK12. As controls we used

12   untransformed YTK12, and YTK12 carrying either Ps87$_{(1-25)}$-pSUC2 (positive control) or

13   Mg87$_{(1-25)}$-pSUC2 (negative control). Yeast strains unable to secrete invertase can grow

14   on SD-Trp medium but not on YPRAA medium.

15

16   **Yeast three-hybrid assays for PNPi, wTGA2.2 and wNPR1.**

17   We used the pBridge vector-based yeast three-hybrid system to test if the presence of

18   PNPi can disrupt the interactions between wTGA2.2 and wNPR1. For these experiments,

19   the full-length wNPR1 was fused with the activation domain (AD) in vector pLAW11

1   (wNPR1-AD). The full-length coding region of wTGA2.2 was fused to the BD in the

2   pBridge vector, whereas a truncated PNPi lacking the signal peptide was expressed under

3   the *M25* promoter as the bridge protein in the same vector (PNPi$_{(23-333)}$^{M25}/wTGA2.2-BD).

4   In this pBridge construct the PNPi$_{(23-333)}$ is not expressed in the presence of Met and is

5   expressed in its absence. As controls, both the full-length wTGA2.2 and the truncated

6   PNPi were expressed as BD fusions in separate pBridge constructs with an empty *M25*

7   promoter (EV^{M25}/wTGA2.2-BD and EV^{M25}/PNPi$_{(23-333)}$-BD, respectively).

8   The resulting wNPR1-AD was co-transformed separately with each of the three

9   pBridge constructs described above into the yeast strain AH109 (Clontech). Clones were

10   first grown on SD-Trp-Leu medium, isolated and diluted equally after counting yeast cell

11   number under the microscope. Aureobasidin A (AbA) at a concentration of 62.5 ng/ml

12   was used as reporter for BD-AD interactions (Clontech) in the Y3H assays. Protein

13   interactions were tested on SD-Leu-Trp +Met +Aba (bridge protein repressed by Met) or

14   SD-Leu-Trp -Met + AbA (bridge protein expressed).

15   The quantitative α-galactosidase assay was used to compare the strength of the

16   interaction between wTGA2.2 and wNPR1 in the presence or absence of the PNPi$_{(23-333)}$

17   bridge protein. Cell populations from PNPi$_{(23-333)}$^{M25}/wTGA2.2-BD and wNPR1-AD were

18   grown to a density of 2–5×10^6 cells ml^{-1} in SD-Leu-Trp +Met and SD-Leu-Trp -Met

19   medium at 30°C. Cells were pelleted using a micro-centrifuge, and an aliquot of 200 μl

20   from the supernatant was mixed with 600 μl of the assay buffer (0.33 M sodium acetate

1   pH 4.5, 33 mM p-nitrophenyl-a-D-galactopyranoside), and was incubated at 30°C for 12–

2   24 h. Reactions were stopped by adding 200 µl of 2 M Na_2CO_3, and activity was

3   measured as the optical density at 410 nm (OD_{410}). We also tested the interaction between

4   wTGA2.2 and PNPi$_{(23-333)}$ in Y2H assays using a wTGA2.2-AD construct from previous

5   research (Cantu et al., 2013a).

6

7   **Evaluation of PNPi-OE, wNPR1-OE and HvNPR1-RNAi barley transgenic lines.**

8   We cloned a truncated *PNPi* gene encoding a protein lacking the signal peptide

9   (PNPi$_{(23-333)}$) under the regulation of the maize *Ubiquitin* promoter in a modified Gateway

10   Binary vector pGWB17. We transformed this construct into the barley variety Golden

11   Promise using *Agrobacterium* at the UC Davis transformation facility

12   (http://ucdptf.ucdavis.edu/). We used a similar approach to generate barley transgenic

13   plants expressing the full-length wheat *wNPR1* transcript under the regulation of the

14   maize *Ubiquitin* promoter (*Ubi::wNPR1*). The primers used to generate the binary vector

15   are described in Supplementary Table S1. We selected three independent transgenic lines

16   overexpressing PNPi and two overexpressing wNPR1 by PCR using primers described in

17   Supplementary Table S1. We used both T_1 and T_2 plants for qRT-PCR assays. RNA

18   interference (RNAi) transgenic barley plants with knockdown expression of *HvNPR1*

19   (*HvNPR1-RNAi*, T_5 homozygous lines) were generously provided by Corina A. Volt

20   (Helmholtz Zentrum Muenchen, Germany) (Dey et al., 2014). Supplementary Table S3

1   summarizes the transgenic lines used in the qRT-PCR assays.

2   Upregulation of the *PR* gene expression was induced by inoculation with *P. syringae*

3   pv. *tomato* DC3000 (Colebrook et al., 2012). Briefly, *P. syringae* DC3000 was grown on

4   King's B medium with *Rif* antibiotics and then diluted to $OD_{600} = 0.2$ in sterile water.

5   Third leaves were inoculated with a 1 ml needless syringe by pressure infiltration of

6   bacterial suspensions through the leaf abaxial surface. The borders of the infiltrated

7   region were marked using a marker pen. Control seedlings were infiltrated in the same

8   way with sterile water. After bacterial inoculation, seedlings were transferred to a

9   constant 23°C condition to facilitate bacterial growth. Samples for qRT-PCR assay were

10   collected from both wild type and transgenic lines from regions adjacent to the

11   infiltration region (~1 cm from the border of the infiltrated region, 48 h post-inoculation).

12   The number of biological replicates used for each transformation event is described in

13   Supplementary Table S3.

14   RNAs were extracted using Sigma Plant total RNA Kit following the manufacturer's

15   instruction and first-strand cDNA was synthesized using the Reverse Transcription kit

16   (Applied Biosystems®). Primers for qRT-PCR are described in Supplementary Table S2.

17   Gene expression was quantified as described before using the barley Elongation Factor

18   1-alphe (*HvEF1a*, Supplementary Table S2) as an internal reference. The *PR* genes

19   induced by *P. syringae* pv. *tomato* DC3000 and characterized by qRT-PCR include

20   *HvPR1b* (Colebrook et al., 2012), *HvPR2* (encoding a β-1-3-glucanase), *HvPR4b*

34

1   (encoding a chitin-binding protein), *HvPR5* (encoding a thaumatin-like protein TLP6),

2   and *HvChitinase 2a* (X78671.1, encoding a Chitinase). The GenBank accessions numbers

3   for the sequences used to design the qRT-PCR primers are listed in Supplementary Table

4   S2.

5   Transcript levels were quantified separately for the different transgenic events and

6   therefore, comparisons were restricted to treatments within the same gene and event. The

7   significance of the differences in expression levels between transgenic and control plants

8   for the different *PR* genes were calculated using SAS program version 9.4. The

9   water-inoculated and *Pseudomonas*-inoculated plants were analyzed separately because

10   the responses were very different. In these statistical analyses the independent transgenic

11   events were used as blocks, separating the variability among events from the analysis of

12   the differences between the wildtype and transgenic plants. This is a stringent analysis

13   because the interaction between Event and Genotype is included in the error term. The

14   figures for PNPi-OE transgenic event 1 are presented in the text as Fig. 5, and those for

15   transgenic events 2, 3 and 4 are presented in the Supplementary Fig. S12. Figures for

16   HvNPR1-RNAi transgenic event 5 and 6 are presented in Supplementary Fig. S14 and

17   those for wNPR1-OE transgenic event 7 and 8 are presented in Supplementary Fig. S15.

18

Page 36 of 80

7

8   **LITERATURE CITED**

9   Besser, K., Jarosch, B., Langen, G., and Kogel, K. H. 2000. Expression analysis of genes

10   induced in barley after chemical activation reveals distinct disease resistance

11   pathways. Mol. Plant Pathol. 1:277-286.

12   Bracha-Drori, K., Shichrur, K., Katz, A., Oliva, M., Angelovici, R., Yalovsky, S., and

13   Ohad, N. 2004. Detection of protein-protein interactions in plants using

14   bimolecular fluorescence complementation. Plant J. 40:419-427.

15   Breen, S., Williams, S. J., Winterberg, B., Kobe, B., and Solomon, P. S. 2016. Wheat

16   PR-1 proteins are targeted by necrotrophic pathogen effector proteins. Plant J.

17   Caillaud, M. C., Asai, S., Rallapalli, G., Piquerez, S., Fabro, G., and Jones, J. D. G. 2013.

18   A downy mildew effector attenuates salicylic acid-triggered immunity in

19   Arabidopsis by interacting with the host mediator complex. PLoS Biol.

20   11:e1001732.

1   Cantu, D., Govindarajulu, M., Kozik, A., Wang, M., Chen, X., Kojima, K., Jurka, J.,

2   Michelmore, R. W., and Dubcovsky, J. 2011. Next generation sequencing

3   provides rapid access to the genome of *Puccinia striiformis* f. sp. *tritici*, the causal

4   agent of wheat stripe rust. PLoS One 6:e24230.

5   Cantu, D., Yang, B., Ruan, R., Li, K., Menzo, V., Fu, D., Chern, M., Ronald, P. C., and

6   Dubcovsky, J. 2013a. Comparative analysis of the defense response interactomes

7   of rice and wheat. BMC Genomics 14:166.

8   Cantu, D., Segovia, V., MacLean, D., Bayles, R., Chen, X. M., Kamoun, S., Dubcovsky,

9   J., Saunders, D. G. O., and Uauy, C. 2013b. Genome analyses of the wheat yellow

10   (stripe) rust pathogen *Puccinia striiformis* f. sp. *tritici* reveal polymorphic and

11   haustorial expressed secreted proteins as candidate effectors. BMC Genomics

12   14:270.

13   Cao, H., Bowling, S. A., Gordon, A. S., and Dong, X. N. 1994. Characterization of an

14   Arabidopsis mutant that is nonresponsive to inducers of systemic

15   acquired-resistance. Plant Cell 6:1583-1592.

16   Cao, H., Glazebrook, J., Clarke, J. D., Volko, S., and Dong, X. N. 1997. The Arabidopsis

17   *NPR1* gene that controls systemic acquired resistance encodes a novel protein

18   containing ankyrin repeats. Cell 88:57-63.

1   Catanzariti, A. M., Dodds, P. N., Lawrence, G. J., Ayliffe, M. A., and Ellis, J. G. 2006.

2   Haustorially expressed secreted proteins from flax rust are highly enriched for

3   avirulence elicitors. Plant Cell 18:243-256.

4   Chen, X. M., Moore, M., Milus, E. A., Long, D. L., Line, R. F., Marshall, D., and Jackson,

5   L. 2002. Wheat stripe rust epidemics and races of *Puccinia striiformis* f. sp. *tritici*

6   in the United States in 2000. Plant Dis. 86:39-46.

7   Chern, M., Canlas, P. E., Fitzgerald, H. A., and Ronald, P. C. 2005a. Rice NRR, a

8   negative regulator of disease resistance, interacts with Arabidopsis NPR1 and rice

9   NH1. Plant J. 43:623-635.

10   Chern, M., Fitzgerald, H. A., Canlas, P. E., Navarre, D. A., and Ronald, P. C. 2005b.

11   Overexpression of a rice NPR1 homolog leads to constitutive activation of

12   defense response and hypersensitivity to light. Mol. Plant Microbe In.

13   18:511-520.

14   Chern, M. S., Fitzgerald, H. A., Yadav, R. C., Canlas, P. E., Dong, X., and Ronald, P. C.

15   2001. Evidence for a disease-resistance pathway in rice similar to the

16   NPR1-mediated signaling pathway in Arabidopsis. Plant J. 27:101-113.

17   Clontech. (2013). Matchmaker® Gold yeast two-hybrid system user manual (Mountain

18   View, CA 94043, USA: Clontech Laboratories, Inc.). 41 pages.

19   Colebrook, E. H., Creissen, G., McGrann, G. R. D., Dreos, R., Lamb, C., and Boyd, L. A.

20   2012. Broad-spectrum acquired resistance in barley induced by the *Pseudomonas*

1   pathosystem shares transcriptional components with Arabidopsis *s*ystemic

2   acquired resistance. Mol. Plant Microbe In. 25:658-667.

3 Delaney, T. P., Friedrich, L., and Ryals, J. A. 1995. Arabidopsis signal-transduction

4   mutant defective in chemically and biologically induced disease resistance. Proc.

5   Natl. Acad. Sci. U.S.A. 92:6602-6606.

6 Després, C., DeLong, C., Glaze, S., Liu, E., and Fobert, P. R. 2000. The arabidopsis

7   NPR1/NIM1 protein enhances the DNA binding activity of a subgroup of the

8   TGA family of bZIP transcription factors. Plant Cell 12:279-290.

9 Després, C., Chubak, C., Rochon, A., Clark, R., Bethune, T., Desveaux, D., and Fobert, P.

10   R. 2003. The Arabidopsis NPR1 disease resistance protein is a novel cofactor that

11   confers redox regulation of DNA binding activity to the basic domain/leucine

12   zipper transcription factor TGA1. Plant Cell 15:2181-2191.

13 Dey, S., Wenig, M., Langen, G., Sharma, S., Kugler, K. G., Knappe, C., Hause, B.,

14   Bichlmeier, M., Babaeizad, V., Imani, J., Janzik, I., Stempfl, T., Huckelhoven, R.,

15   Kogel, K. H., Mayer, K. F. X., and Vlot, A. C. 2014. Bacteria-triggered systemic

16   immunity in barley is associated with WRKY and ETHYLENE RESPONSIVE

17   FACTORs but not with salicylic acid. Plant Physiol. 166:2133-2151.

18 Djamei, A., Schipper, K., Rabe, F., Ghosh, A., Vincon, V., Kahnt, J., Osorio, S., Tohge, T.,

19   Fernie, A. R., Feussner, I., Feussner, K., Meinicke, P., Stierhof, Y. D., Schwarz, H.,

1   Macek, B., Mann, M., and Kahmann, R. 2011. Metabolic priming by a secreted

2   fungal effector. Nature 478:395-398.

3   Dou, D. L., Kale, S. D., Wang, X., Jiang, R. H. Y., Bruce, N. A., Arredondo, F. D., Zhang,

4   X. M., and Tyler, B. M. 2008. RXLR-mediated entry of *Phytophthora sojae*

5   effector Avr1b into soybean cells does not require pathogen-encoded machinery.

6   Plant Cell 20:1930-1947.

7   Fan, W. H., and Dong, X. N. 2002. In vivo interaction between NPR1 and transcription

8   factor TGA2 leads to salicylic acid-mediated gene activation in Arabidopsis. Plant

9   Cell 14:1377-1389.

10   Feng, J. X., Cao, L., Li, J., Duan, C. J., Luo, X. M., Le, N., Wei, H. H., Liang, S. J., Chu,

11   C. C., Pan, Q. H., and Tang, J. L. 2011. Involvement of OsNPR1/NH1 in rice

12   basal resistance to blast fungus *Magnaporthe oryzae*. Eur. J. Plant Pathol.

13   131:221-235.

14   Finn, R. D., Bateman, A., Clements, J., Coggill, P., Eberhardt, R. Y., Eddy, S. R., Heger,

15   A., Hetherington, K., Holm, L., Mistry, J., Sonnhammer, E. L. L., Tate, J., and

16   Punta, M. 2014. Pfam: the protein families database. Nucleic Acids Res.

17   42:D222-D230.

18   Fu, Z. Q., and Dong, X. 2013. Systemic acquired resistance: turning local infection into

19   global defense. Annu. Rev. Plant Biol. 64:839-863.

1   Fu, Z. Q., Yan, S. P., Saleh, A., Wang, W., Ruble, J., Oka, N., Mohan, R., Spoel, S. H.,

2   Tada, Y., Zheng, N., and Dong, X. N. 2012. NPR3 and NPR4 are receptors for the

3   immune signal salicylic acid in plants. Nature 486:228-233.

4   Ganesan, V., and Thomas, G. 2001. Salicylic acid response in rice: influence of salicylic

5   acid on H_2O_2 accumulation and oxidative stress. Plant Sci. 160:1095-1106.

6   Gangadharan, A., Sreerekha, M. V., Whitehill, J., Ham, J. H., and Mackey, D. 2013. The

7   *Pseudomonas syringae* pv. *tomato* Type III effector HopM1 suppresses

8   Arabidopsis defenses independent of suppressing salicylic acid signaling and of

9   targeting AtMIN7. PLoS One 8:e82032.

10 Garnica, D. P., Upadhyaya, N. M., Dodds, P. N., and Rathjen, J. P. 2013. Strategies for

11   wheat stripe rust pathogenicity identified by transcriptome sequencing. PLoS One

12   8:e67150.

13 Gietz, R. D., and Woods, R. A. 2002. Transformation of yeast by lithium

14   acetate/single-stranded carrier DNA/polyethylene glycol method. Method

15   Enzymol. 350:87-96.

16 Görlach, J., Volrath, S., KnaufBeiter, G., Hengy, G., Beckhove, U., Kogel, K. H.,

17   Oostendorp, M., Staub, T., Ward, E., Kessmann, H., and Ryals, J. 1996.

18   Benzothiadiazole, a novel class of inducers of systemic acquired resistance,

19   activates gene expression and disease resistance in wheat. Plant Cell 8:629-643.

1   Gu, B. A., Kale, S. D., Wang, Q. H., Wang, D. H., Pan, Q. N., Cao, H., Meng, Y. L., Kang,

2   Z. S., Tyler, B. M., and Shan, W. X. 2011. Rust secreted protein Ps87 is conserved

3   in diverse fungal pathogens and contains a RXLR-like motif sufficient for

4   translocation into plant cells. PLoS One 6:e27217.

5   Guttman, D. S., McHardy, A. C., and Schulze-Lefert, P. 2014. Microbial genome-enabled

6   insights into plant-microorganism interactions. Nat. Rev. Genet. 15:797-813.

7   Hofgen, R., and Willmitzer, L. 1988. Storage of competent cells for *Agrobacterium*

8   transformation. Nucleic Acids Res. 16:9877-9877.

9   Hovmøller, M. S., Walter, S., and Justesen, A. F. 2010. Escalating threat of wheat rusts.

10   Science 329:369-369.

11   Hovmøller, M. S., Walter, S., Bayles, R. A., Hubbard, A., Flath, K., Sommerfeldt, N.,

12   Leconte, M., Czembor, P., Rodriguez-Algaba, J., Thach, T., Hansen, J. G., Lassen,

13   P., Justesen, A. F., Ali, S., and de Vallavieille-Pope, C. 2016. Replacement of the

14   European wheat yellow rust population by new races from the centre of diversity

15   in the near-Himalayan region. Plant Pathol. 65:402-411.

16   Johnson, C., Boden, E., and Arias, J. 2003. Salicylic acid and NPR1 induce the

17   recruitment of trans-activating TGA factors to a defense gene promoter in

18   Arabidopsis. Plant Cell 15:1846-1858.

19   Jones, J. D. G., and Dangl, J. L. 2006. The plant immune system. Nature 444:323-329.

1   Kale, S. D., and Tyler, B. M. 2011. Entry of oomycete and fungal effectors into plant and

2   animal host cells. Cell Microbiol. 13:1839-1848.

3   Kale, S. D., Gu, B. A., Capelluto, D. G. S., Dou, D. L., Feldman, E., Rumore, A.,

4   Arredondo, F. D., Hanlon, R., Fudal, I., Rouxel, T., Lawrence, C. B., Shan, W. X.,

5   and Tyler, B. M. 2010. External lipid PI3P mediates entry of eukaryotic pathogen

6   effectors into plant and animal host cells. Cell 142:284-295.

7   Kazan, K., and Lyons, R. 2014. Intervention of phytohormone pathways by pathogen

8   effectors. Plant Cell 26:2285-2309.

9   Kinkema, M., Fan, W. H., and Dong, X. N. 2000. Nuclear localization of NPR1 is

10   required for activation of *PR* gene expression. Plant Cell 12:2339-2350.

11   Kogel, K. H., Beckhove, U., Dreschers, J., Munch, S., and Romme, Y. 1994.

12   Acquired-resistance in barley - the resistance mechanism induced by

13   2,6-dichloroisonicotinic acid is a phenocopy of a genetically based mechanism

14   governing race-specific powdery mildew resistance. Plant Physiol.

15   106:1269-1277.

16   Krasileva, K. V., Buffalo, V., Bailey, P., Pearce, S., Ayling, S., Tabbita, F., Soria, M.,

17   Wang, S., Consortium, I., Akhunov, E., Uauy, C., and Dubcovsky, J. 2013.

18   Separating homeologs by phasing in the tetraploid wheat transcriptome. Genome

19   Biol. 14:R66.

1 Li, C., Lin, H., and Dubcovsky, J. 2015. Factorial combinations of protein interactions

2   generate a multiplicity of florigen activation complexes in wheat and barley. Plant

3   J. 84:70-82.

4 Maccaferri, M., Zhang, J., Bulli, P., Abate, Z., Chao, S., Cantu, D., Bossolini, E., Chen,

5   X., Pumphrey, M., and Dubcovsky, J. 2015. A genome-wide association study of

6   resistance to stripe rust (*Puccinia striiformis* f. sp. *tritici*) in a worldwide

7   collection of hexaploid spring wheat (*Triticum aestivum* L.). G3 (Bethesda)

8   5:449-465.

9 Makandar, R., Essig, J. S., Schapaugh, M. A., Trick, H. N., and Shah, J. 2006. Genetically

10   engineered resistance to *Fusarium* head blight in wheat by expression of

11   Arabidopsis NPR1. Mol. Plant Microbe In. 19:123-129.

12 Michelmore, R., Christopoulou, M., and Caldwell, K. S. 2013. Impacts of resistance gene

13   genetics, function, and evolution on a durable future. Annu. Rev. Phytopathol.

14   51:291-319.

15 Molina, A., Gorlach, J., Volrath, S., and Ryals, J. 1999. Wheat genes encoding two types

16   of PR-1 proteins are pathogen inducible, but do not respond to activators of

17   systemic acquired resistance. Mol. Plant Microbe In. 12:53-58.

18 Moller, S., Croning, M. D. R., and Apweiler, R. 2001. Evaluation of methods for the

19   prediction of membrane spanning regions. Bioinformatics 17:646-653.

1   Moreau, M., Tian, M. Y., and Klessig, D. F. 2012. Salicylic acid binds NPR3 and NPR4

2   to regulate NPR1-dependent defense responses. Cell Res. 22:1631-1633.

3   Mou, Z., Fan, W. H., and Dong, X. N. 2003. Inducers of plant systemic acquired

4   resistance regulate NPR1 function through redox changes. Cell 113:935-944.

5   Petersen, T. N., Brunak, S., von Heijne, G., and Nielsen, H. 2011. SignalP 4.0:

6   discriminating signal peptides from transmembrane regions. Nat. Methods

7   8:785-786.

8   Petre, B., and Kamoun, S. 2014. How do filamentous pathogens deliver effector proteins

9   into plant cells? PLoS Biol. 12:2798.

10   Petre, B., Kopischke, M., Evrard, A., Robatzek, S., and Kamoun, S. 2016. Cell re-entry

11   assays do not support models of pathogen-independent translocation of AvrM and

12   AVR3a effectors into plant cells. bioRxiv doi: http://dx.doi.org/10.1101/038232.

13   Petre, B., Saunders, D. G. O., Sklenar, J., Lorrain, C., Krasileva, K. V., Win, J., Duplessis,

14   S., and Kamoun, S. 2015. In planta expression screens of candidate effector

15   proteins from the wheat yellow rust fungus reveal processing bodies as a

16   pathogen-targeted plant cell compartment. BioRxiv doi:

17   dx.doi.org/10.1101/032276.

18   Petroski, M. D., and Deshaies, R. J. 2005. Function and regulation of cullin-RING

19   ubiquitin ligases. Nat. Rev. Mol. Cell Bio. 6:9-20.

1   Raffaele, S., and Kamoun, S. 2012. Genome evolution in filamentous plant pathogens:

2   why bigger can be better. Nat. Rev. Microbiol. 10:417-430.

3   Rafiqi, M., Gan, P. H. P., Ravensdale, M., Lawrence, G. J., Ellis, J. G., Jones, D. A.,

4   Hardham, A. R., and Dodds, P. N. 2010. Internalization of flax rust avirulence

5   proteins into flax and tobacco cells can occur in the absence of the pathogen.

6   Plant Cell 22:2017-2032.

7   Ravensdale, M., Bernoux, M., Ve, T., Kobe, B., Thrall, P. H., Ellis, J. G., and Dodds, P. N.

8   2012. Intramolecular interaction influences binding of the flax L5 and L6

9   resistance proteins to their AvrL567 ligands. PLoS Path. 8:e1003004.

10   Ryals, J., Weymann, K., Lawton, K., Friedrich, L., Ellis, D., Steiner, H. Y., Johnson, J.,

11   Delaney, T. P., Jesse, T., Vos, P., and Uknes, S. 1997. The Arabidopsis NIM1

12   protein shows homology to the mammalian transcription factor inhibitor I kappa

13   B. Plant Cell 9:425-439.

14   Schütze, K., Harter, K., and Chaban, C. 2009. Bimolecular fluorescence complementation

15   (BiFC) to study protein-protein interactions in living plant cells. Methods Mol.

16   Biol. 479:189-202.

17   Sedgwick, S. G., and Smerdon, S. J. 1999. The ankyrin repeat: a diversity of interactions

18   on a common structural framework. Trends Biochem. Sci. 24:311-316.

1   Shah, J., Tsui, F., and Klessig, D. F. 1997. Characterization of a salicylic acid-insensitive

2   mutant (*sai1*) of *Arabidopsis thaliana*, identified in a selective screen utilizing the

3   SA-inducible expression of the *tms2* gene. Mol. Plant Microbe In. 10:69-78.

4   Simons, K., Abate, Z., Chao, S. M., Zhang, W. J., Rouse, M., Jin, Y., Elias, E., and

5   Dubcovsky, J. 2011. Genetic mapping of stem rust resistance gene *Sr13* in

6   tetraploid wheat (*Triticum turgidum* ssp. *durum* L.). Theor. Appl. Genet.

7   122:649-658.

8   Sugano, S., Jiang, C. J., Miyazawa, S. I., Masumoto, C., Yazawa, K., Hayashi, N.,

9   Shimono, M., Nakayama, A., Miyao, M., and Takatsuji, H. 2010. Role of

10   OsNPR1 in rice defense program as revealed by genomewide expression analysis.

11   Plant Mol. Biol. 74:549-562.

12   Sun, F. R., Kale, S. D., Azurmendi, H. F., Li, D., Tyler, B. I., and Capelluto, D. G. S. 2013.

13   Structural basis for interactions of the *Phytophthora sojae* RxLR effector Avh5

14   with phosphatidylinositol 3-phosphate and for host cell entry. Mol. Plant Microbe

15   In. 26:330-344.

16   Tamura, K., Stecher, G., Peterson, D., Filipski, A., and Kumar, S. 2013. MEGA6:

17   Molecular evolutionary genetics analysis version 6.0. Mol. Biol. Evol.

18   30:2725-2729.

19   Tyler, B. M., Kale, S. D., Wang, Q. Q., Tao, K., Clark, H. R., Drews, K., Antignani, V.,

20   Rumore, A., Hayes, T., Plett, J. M., Fudal, I., Gu, B., Chen, Q. H., Affeldt, K. J.,

Berthier, E., Fischer, G. J., Dou, D. L., Shan, W. X., Keller, N. P., Martin, F., Rouxel, T., and Lawrence, C. B. 2013. Microbe-independent entry of oomycete RxLR effectors and fungal RxLR-like effectors into plant and animal cells is specific and reproducible. Mol. Plant Microbe In. 26:611-616.

Üstün, S., Bartetzko, V., and Bornke, F. 2013. The X*anthomonas campestris* Type III effector XopJ targets the host cell proteasome to suppress salicylic-acid mediated plant defence. PLoS Path. 9:e1003427.

Vallelian-Bindschedler, L., Metraux, J. P., and Schweizer, P. 1998. Salicylic acid accumulation in barley is pathogen specific but not required for defense-gene activation. Mol. Plant Microbe In. 11:702-705.

Voegele, R. T., Struck, C., Hahn, M., and Mendgen, K. 2001. The role of haustoria in sugar supply during infection of broad bean by the rust fungus *Uromyces fabae*. Proc. Natl. Acad. Sci. U.S.A. 98:8133-8138.

Wang, Q. Q., Han, C. Z., Ferreira, A. O., Yu, X. L., Ye, W. W., Tripathy, S., Kale, S. D., Gu, B. A., Sheng, Y. T., Sui, Y. Y., Wang, X. L., Zhang, Z. G., Cheng, B. P., Dong, S. M., Shan, W. X., Zheng, X. B., Dou, D. L., Tyler, B. M., and Wang, Y. C. 2011. Transcriptional programming and functional interactions within the *Phytophthora sojae* RXLR effector repertoire. Plant Cell 23:2064-2086.

Wang, X. D., Wang, X. J., Deng, L., Chang, H. T., Dubcovsky, J., Feng, H., Han, Q. M., Huang, L. L., and Kang, Z. S. 2014. Wheat TaNPSN SNARE homologues are

1   involved in vesicle-mediated resistance to stripe rust (*Puccinia striiformis* f. sp.

2   *tritici*). J. Exp. Bot. 65:4807-4820.

3 Wawra, S., Djamei, A., Albert, I., Nurnberger, T., Kahmann, R., and van West, P. 2013. In

4   vitro translocation experiments with RxLR-reporter fusion proteins of Avr1b from

5   *Phytophthora sojae* and AVR3a from *Phytophthora infestans* fail to demonstrate

6   specific autonomous uptake in plant and animal cells. Mol. Plant Microbe In.

7   26:528-536.

8 Wu, Y., Zhang, D., Chu, J. Y., Boyle, P., Wang, Y., Brindle, I. D., De Luca, V., and

9   Despres, C. 2012. The Arabidopsis NPR1 protein is a receptor for the plant

10   defense hormone salicylic acid. Cell Rep. 1:639-647.

11 Yang, B., Ruan, R., Cantu, D., Wang, X., Ji, W., Ronald, P. C., and Dubcovsky, J. 2013. A

12   comparative approach expands the protein-protein interaction node of the immune

13   receptor *XA21* in wheat and rice. Genome 56:315-326.

14 Yuan, Y. X., Zhong, S. H., Li, Q., Zhu, Z. R., Lou, Y. G., Wang, L. Y., Wang, J. J., Wang,

15   M. Y., Li, Q. L., Yang, D. L., and He, Z. H. 2007. Functional analysis of rice

16   NPR1-like genes reveals that OsNPR1/NH1 is the rice orthologue conferring

17   disease resistance with enhanced herbivore susceptibility. Plant Biotechnol. J.

18   5:313-324.

19 Zhang, W. J., Pedersen, C., Kwaaitaal, M., Gregersen, P. L., Morch, S. M., Hanisch, S.,

20   Kristensen, A., Fuglsang, A. T., Collinge, D. B., and Thordal-Christensen, H. 2012.

1   Interaction of barley powdery mildew effector candidate CSEP0055 with the

2   defence protein PR17c. Mol. Plant Pathol. 13:1110-1119.

3   Zhang, Y. L., Fan, W. H., Kinkema, M., Li, X., and Dong, X. N. 1999. Interaction of

4   NPR1 with basic leucine zipper protein transcription factors that bind sequences

5   required for salicylic acid induction of the *PR-1* gene. Proc. Natl. Acad. Sci.

6   U.S.A. 96:6523-6528.

7   Zheng, W. M., Huang, L. L., Huang, J. Q., Wang, X. J., Chen, X. M., Zhao, J., Guo, J.,

8   Zhuang, H., Qiu, C. Z., Liu, J., Liu, H. Q., Huang, X. L., Pei, G. L., Zhan, G. M.,

9   Tang, C. L., Cheng, Y. L., Liu, M., Zhang, J. S., Zhao, Z. T., Zhang, S. J., Han, Q.

10   M., Han, D. J., Zhang, H. C., Zhao, J., Gao, X. N., Wang, J. F., Ni, P. X., Dong,

11   W., Yang, L. F., Yang, H. M., Xu, J. R., Zhang, G. Y., and Kang, Z. S. 2013. High

12   genome heterozygosity and endemic genetic recombination in the wheat stripe

13   rust fungus. Nat. Commun. 4:2673.

14

15   **FIGURE LEGENDS**

16   **Fig. 1.** Sequence alignment of PNPi proteins from different cereal rust pathogens.

17   Multi-sequence alignment performed using MUSCLE showing conservation among PNPi

18   homologs from *Puccinia striiformis* f. sp. *hordei* (*Psh*), *Puccinia striiformis* f. sp. *tritici*

19   (*Pst*), *Puccinia graminis* f. sp. *tritici* (*Pgt)* and *Puccinia triticina* (*Pt*). The predicted

20   proteins include an N-terminal signal peptide followed by a RxLR-dEER-like motif, and

1   a C-terminal region including a DPBB_1 domain.

2

3   **Fig. 2.** wNPR1, wNPR3, wNPR4 and PNPi interactions in yeast two-hybrid assays. **A,**

4   Domain predictions for wheat wNPR1, wNPR3, and wNPR4 and *Pst* PNPi using Pfam.

5   Segments indicated in black were cloned into Y2H vectors. **B,** Yeast two-hybrid assays to

6   assess domain interaction between PNPi and wNPR1, wNPR3 and wNPR4. Yeast

7   transformants co-expressing different bait and prey constructs were assayed on

8   SD-Leu-Trp-His and SD-Leu-Trp-His-Ade. PNPi specifically interacted with

9   NPR1/NIM1-like domain from wNPR1 via its DPBB_1 domain. PNPi also showed

10   interaction with Arabidopsis NPR1 and NPR1/NIM1-like domain from wNPR4 but not

11   wNPR3.

12

13   **Fig. 3.** Bimolecular fluorescence complementation assays. Bimolecular fluorescence

14   complementation assays showed interaction between YFP^N-PNPi$_{(23-333)}$ and

15   YFP^C-wNPR1 in *N. benthamiana* protoplast. YFP^N-wHSP90.3 and YFP^C-wRAR1 were

16   used as positive control. Co-expression of each recombinant vector with its

17   corresponding non-fused YFP^N and YFP^C empty vectors served as negative controls. BF

18   = bright field; EV = empty vector; YFP = yellow fluorescent protein. Scale bars = 100

19   μm.

20

1   **Fig. 4.** Yeast three-hybrid assay to determine the effect of competing PNPi$_{(23-333)}$ protein

2   on the interactions between wTGA2.2 and wNPR1. **A,** Yeast transformants co-expressing

3   EV^{M25}/wTGA2.2-BD, EV^{M25}/PNPi$_{(23-333)}$-BD or PNPi$_{(23-333)}$^{M25}/wTGA2.2-BD with

4   wNPR1-pGADT7. Left panels without Aba (with and without Met) were used to

5   normalize yeast cell number. Yeast transformants were assayed on SD-Leu-Trp +Aba

6   medium with and without Met. The interaction between wTGA2.2 and wNPR1 was

7   weaker in the presence of PNPi$_{(23-333)}$ (-Met) than in its absence (+Met). EV = empty

8   vector site; Met = Methionine; Aba = Aureobasidin. **B,** Yeast transformants were then

9   assayed on SD-Leu-Trp-Met+X-α-Gal$_{40}$ selection medium. The blue color intensity of the

10   wTGA2.2-BD interaction with wNPR1-AD in the presence of PNPi$_{(23-333)}$^{M25} was weaker

11   than in the absence of the putative effector (EV^{M25}/wTGA2.2-BD). **C,** Quantitative α-gal

12   assay showed that the interaction between wTGA and wNPR1 was significantly reduced

13   in the presence of PNPi$_{(23-333)}$ (** = $P < 0.01$). Relative α-galactosidase activity values for

14   each interaction were the average of six replicates (error bars = Standard Error). EV =

15   empty vector.

16

17   **Fig. 5.** Functional characterization of PNPi$_{(23-333)}$. **A,** Infiltration of young barley leaves

18   with either *Pseudomonas syringae* pv. *tomato* DC3000 or sterile water as control. The

19   borders of the infiltrated region were marked in black. Samples for qRT-PCR assays were

20   collected from the leaf region adjacent to the infection 48 hours after inoculation. **B-F,**

1   Relative expression of antimicrobial *PR* genes *HvPR1b*, *HvPR2*, *HvPR4b*, *HvPR5* and

2   *HvChitinase 2a* genes was measured by qRT-PCR in the region adjacent to the

3   inoculation. Data for Event 1 is presented in this figure and events 2, 3 and 4 in

4   Supplementary Fig. S5. The Y scale indicates transcript levels relative to barley

5   endogenous control *HvEF1a*. *P* values indicated below the water and DC3000 treatments

6   indicate significance of the differences between transgenic and control plants in

7   combined ANOVAs using transgenic events as blocks. Error bars indicate standard error

8   of the means calculated from eight independent biological replicates.

9

10

11   **SUPPLEMENTARY MATERIALS**

12   **Supplementary Tables**

13   **Supplementary Table S1.** Primers for cloning, yeast two- and three-hybrid assays,

14   subcellular localization, and constructs for PNPi transgenic plants.

15   **Supplementary Table S2.** Primers used for qRT-PCR expression studies.

16   **Supplementary Table S3.** Transgenic lines used in qRT-PCR assays.

17

18   **Supplementary Figures**

19   **Supplementary Fig. S1.** Alignments of DPBB_1 domains from PNPi homologs.

20   **Supplementary Fig. S2.** Neighbor-joining tree for PNPi and closest homologs from

1   other plant pathogens.

2   **Supplementary Fig. S3.** Expression of *PNPi* during PST130 infection.

3   **Supplementary Fig. S4.** Negative controls for Y2H assay.

4   **Supplementary Fig. S5.** Western blot validation of protein expression in yeast

5   two-hybrid assays with negative results.

6   **Supplementary Fig. S6.** Amino acid substitutions in PNPi and their effect on the

7   interactions with wNPR1 in yeast two-hybrid assays.

8   **Supplementary Fig. S7.** Negative controls for BiFC assays.

9   **Supplementary Fig. S8.** Western blot validation of protein expression in BiFC assays.

10   **Supplementary Fig. S9.** Functional validation of PNPi predicted signal peptides using a

11   yeast invertase secretion assay.

12   **Supplementary Fig. S10.** Subcellular localization of PNPi in *N. benthamiana* epidermal

13   cells.

14   **Supplementary Fig. S11.** Transcript levels of *PNPi* in different *Ubi::PNPi* transgenic

15   events in barley.

16   **Supplementary Fig. S12.** Functional characterization of transgenic barley lines

17   overexpressing *PNPi* (*PNPi-OE*).

18   **Supplementary Fig. S13.** Transcript levels of NPR1 in *Ubi::wNPR1* (overexpression)

19   and *HvNPR1-RNAi* (downregulation) in barley transgenic plants.

20   **Supplementary Fig. S14.** Transcript levels of *PR* genes in *HvNPR1-RNAi* transgenic

1	barley plants.

2	**Supplementary Fig. S15.** Transcript levels of *PR* genes in *Ubi::wNPR1* transgenic

3	barley plants.

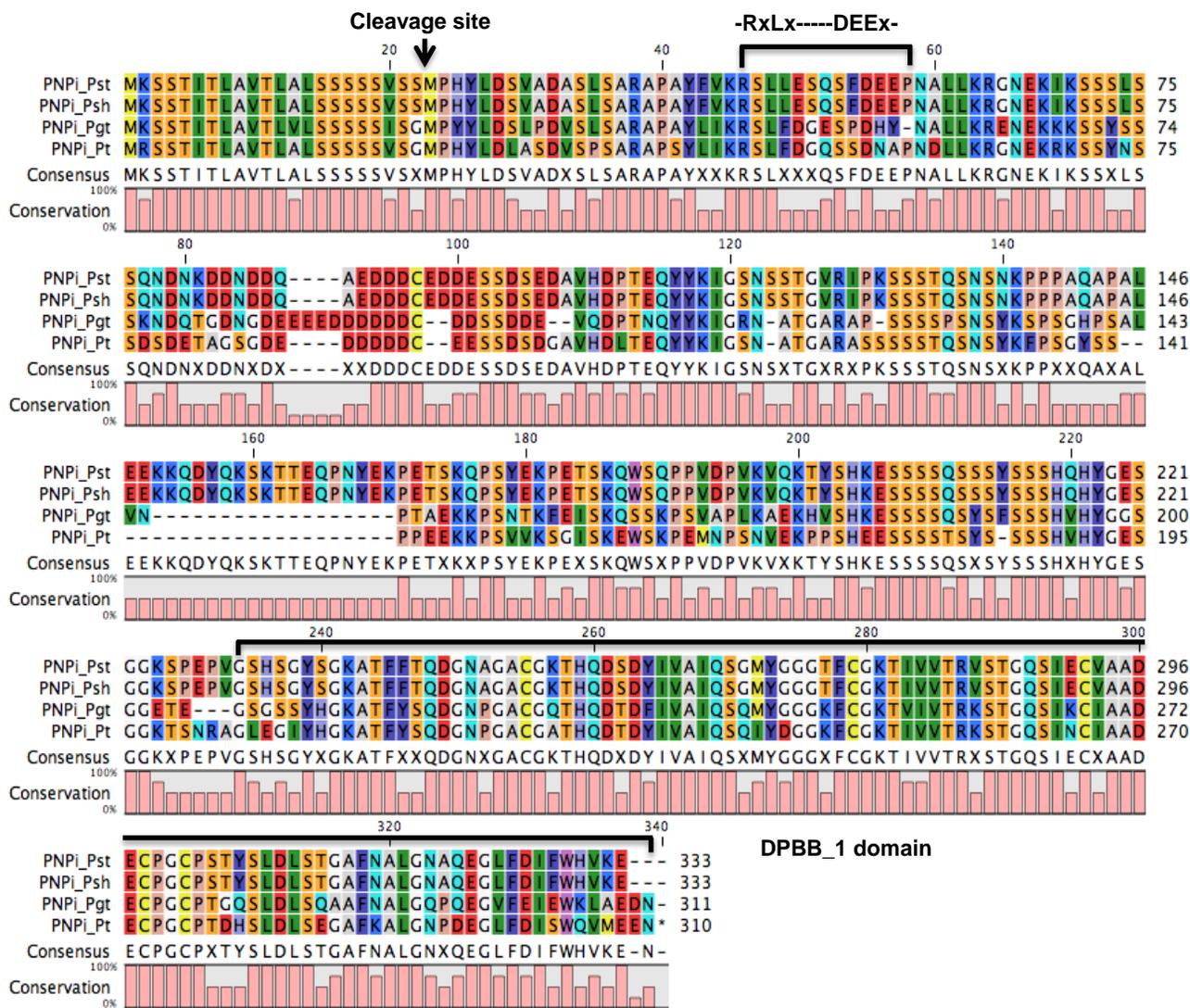4	**Supplementary Fig. S16.** Comparison of NPR1 proteins.

Figure 1

A

wNPR1 — BTB/POZ DUF3420 ANK NPR1/NIM1-like
1-170aa 196-363aa 355-572aa

wNPR3 — BTB/POZ ANK NPR1/NIM1-like
373-593aa

wNPR4 — BTB/POZ ANK NPR1/NIM1-like
385-607aa

PNPi — Signal Peptide DPBB_1
23-235aa 236-333aa

B

AD / BD

SD-Leu-Trp-His   SD-Leu-Trp-His-Ade
1:1 1:10 1:100   1:1 1:10 1:100

wNPR1/PNPi(23-333)
AtNPR1/PNPi(23-333)
wNPR1/PNPi(23-235)
wNPR1/PNPi(236-333)
wNPR1(1-170)/PNPi(23-333)
wNPR1(196-363)/PNPi(23-333)
wNPR1(355-572)/PNPi(23-333)
wNPR1(1-170)/PNPi(236-333)
wNPR1(196-363)/PNPi(236-333)
wNPR1(355-572)/PNPi(236-333)
wNPR3(373-593)/PNPi(23-333)
wNPR4(385-607)/PNPi(23-333)
wTGA2.2/PNPi(23-333)
Positive
Negative

Figure 2

	YFP	BF	YFP/BF
YFP^N-wHSP90.3 / YFP^C-wRAR1			
YFP^N-PNPi$_{(23-333)}$ / YFP^C-wNPR1			
YFP^N-PNPi$_{(23-333)}$ / YFP^C-EV			
YFP^N-EV / YFP^C-wNPR1			
YFP^N-EV / YFP^C-EV			

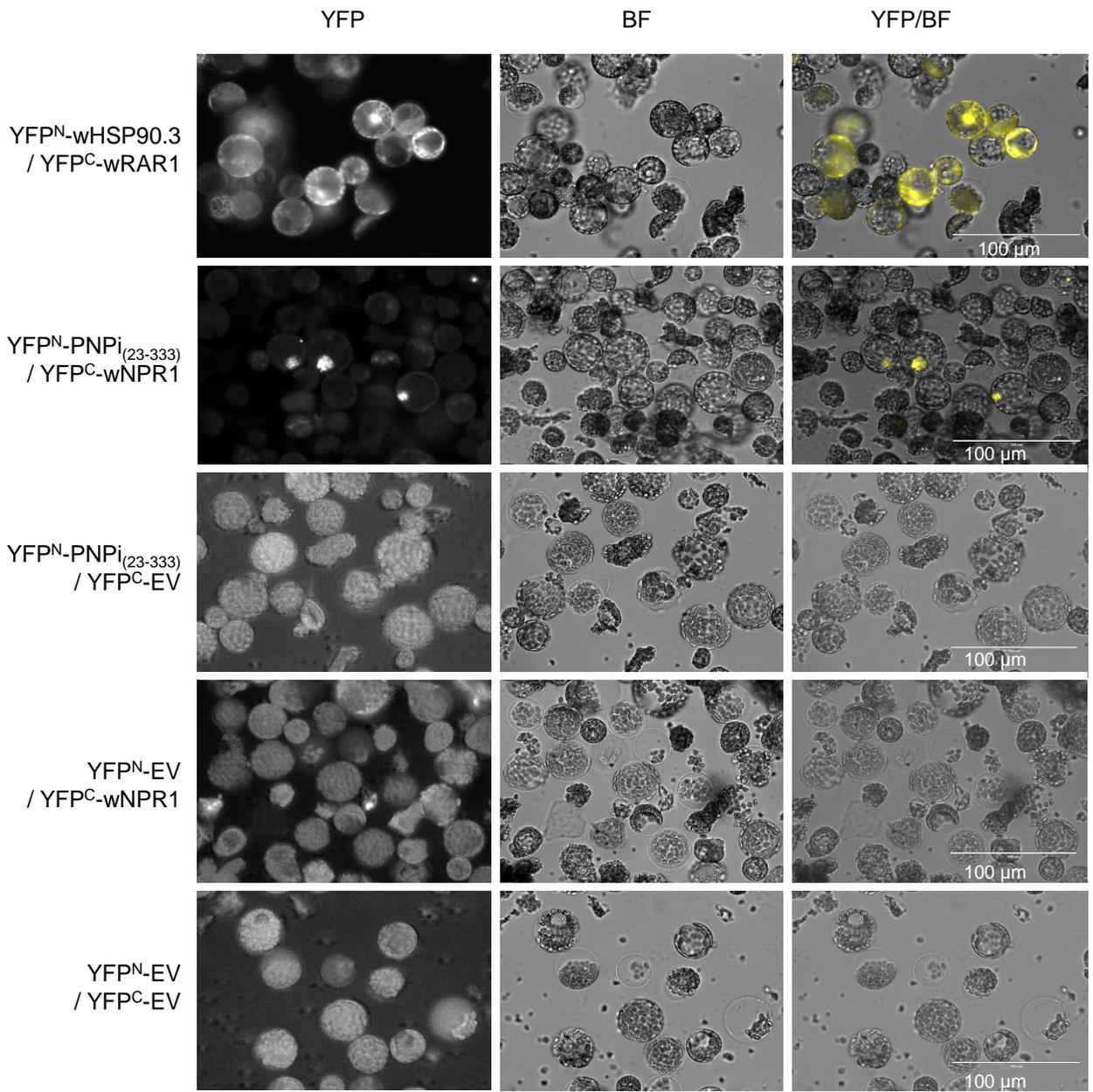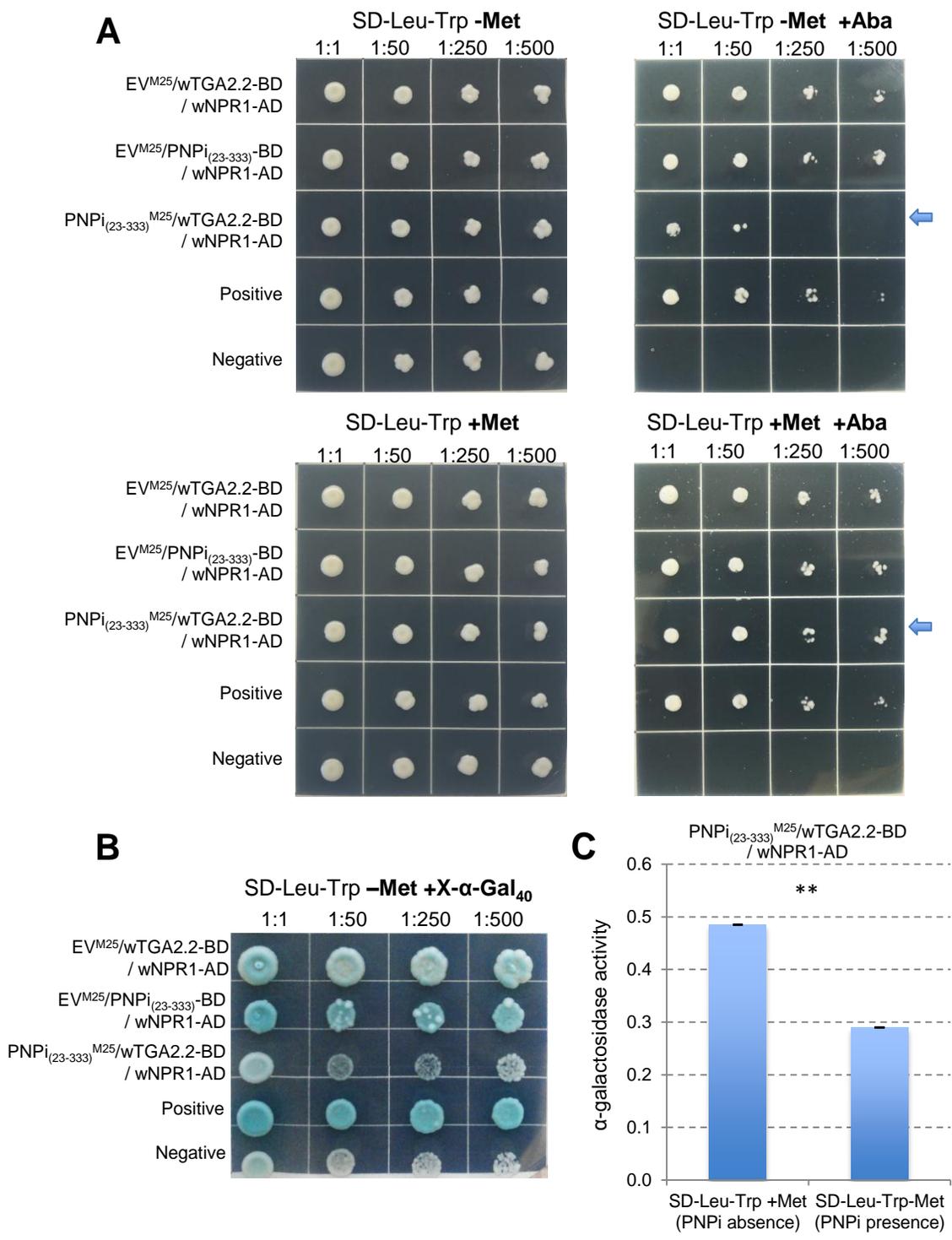**Figure 3**

Figure 4

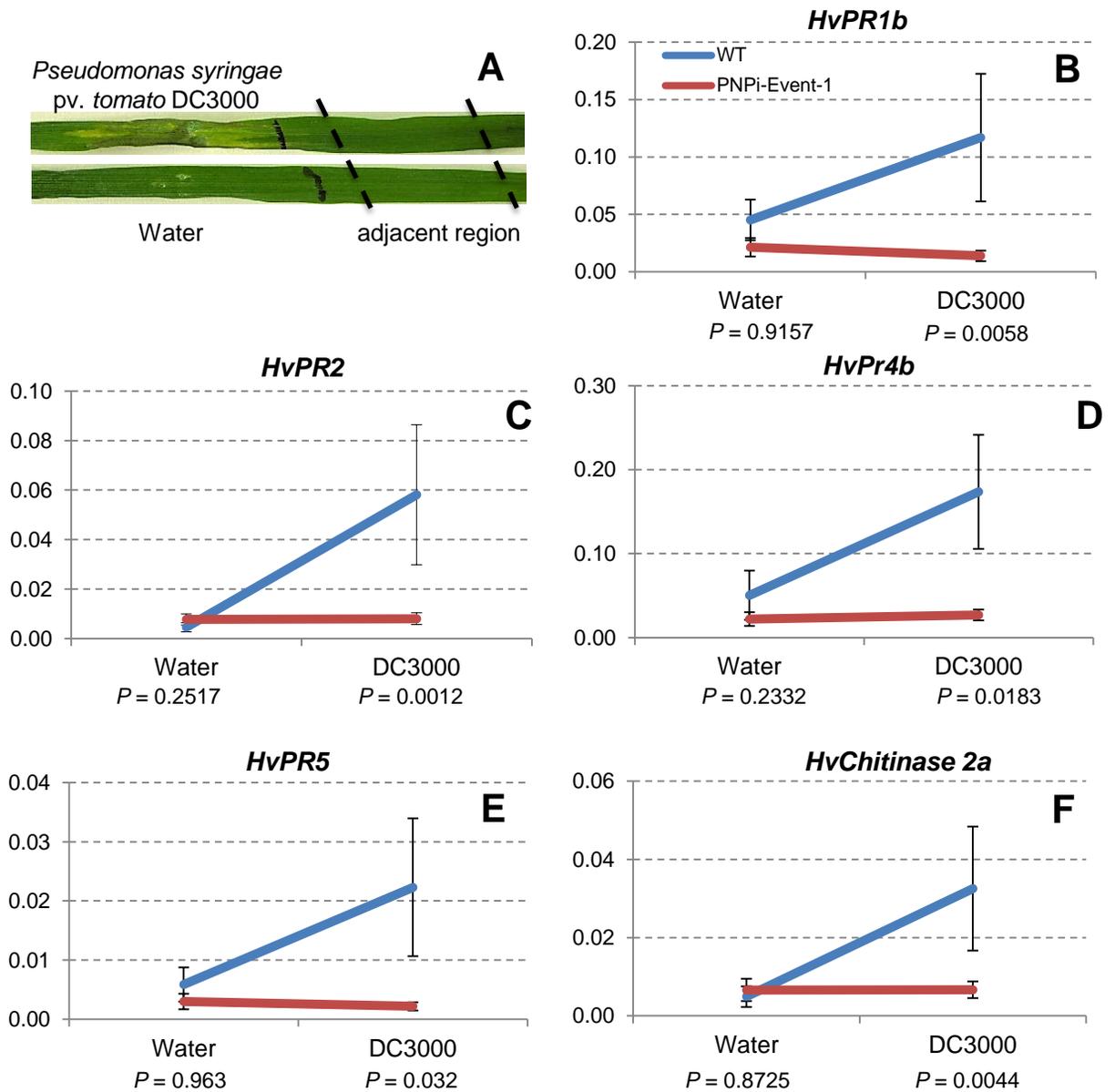Figure 5

Supplementary Tables

Supplementary Table S1. Primers for cloning, yeast two- and three-hybrid assays, subcellular localization and constructs for PNPi transgenic plants.

| Function	Name	Sequence 5' to 3'	bp
Y2H Screening	AD-F	CTATTCGATGATGAAGATACCCCACCAAACCC	
	AD-R	GTGAACTTGCGGGGTTTTTCAGTATCTACGAT	
Cloning of PNPi	PNPi-ORF-F	caccATGAAGTCGTCGACCATCACTCT	1002
	PNPi-ORF-R	TTCTTTGACATGCCAGAGGATA	
	PNPi-nSP-F	caccATGCCGCACTACCTTGACTC	933
	PNPi-nSP-R	TTCTTTGACATGCCAGAGGATA	
	PNPi(23-235)-Y2H-F	caccATGCCGCACTACCTTGACT	639
	PNPi(23-235)-Y2H-R	ATAACCGCTGTGTGATCCC	
	PNPi(236-333)-Y2H-F	caccAGCGGAAAAGCCACTTTCTTTAC	297
	PNPi(236-333)-Y2H-R	TTCTTTGACATGCCAGAGGATA	
	wNPR1-Y2H-F	caccATGGAGGCCCCGAGCAGC	1734
	wNPR1-Y2H-R	TCTCCTAGGCCGGCCTGT	
	wNPR1(1-170aa)-Y2H-F	caccATGGAGGCCCCGAGCAGCCACGTCA	513
	wNPR1(1-170aa)-Y2H-R	GACCTGGAAGGTGGATGC	
Yeast two-hybrid assays	wNPR1(196-363aa)-Y2H-F	caccTTGATCTTATCTGTTGCAAACTTAT	504
	wNPR1(196-363aa)-Y2H-R	TTGAACTGCTTTTCTTCCATC	
	wNPR1(355-572aa)-Y2H-F	caccTTTGATGGAAGAAAAGCAGTT	651
	wNPR1(355-572aa)-Y2H-R	TGTCAAGTTCCTTGCTACAGTG	
	wNPR3(373-593aa)-Y2H-F	caccGCGCTTACCATCTGCAAGAGA	660
	wNPR3(373-593aa)-Y2H-R	ATGTCTACTAACCTTTCCATCACCTCT	
	wNPR4(385-607aa)-Y2H-F	caccGCGTCGCAATTGACAGATG	666
	wNPR4(385-607aa)-Y2H-R	CCCCGAGGATGAGGAGTTT	
Yeast three-hybrid assays	PNPi-Y3H-F	ATAAGAATGCGGCCGCATGAAGTCGTCGACCATC	933
	PNPi-Y3H-R	CCTAGATCTTTCTTTGACATGCCAGAGGATA	
	wTGA2-Y3H-F	CGCGGATCCATGGCTGATGCTAGTTCGAG	1005

	wTGA2-Y3H-R	AAGGCGCCGGCGATACCGGCTGGTCGACCTCCCGTGGCCTCGCAAG	
Signal peptide and N-terminal subcellular localization	PNPi(1-64)-F	caccATGAAGTCGTCGACCATCACTC	192
	PNPi(1-64)-R	CCGTTTGAGAAGAGCGTTAGG	
	PNPi(1-22)-F	caccATGAAGTCGTCGACCATCACTC	66
	PNPi(1-22)-R	ACTCGAGACGGATGATGAG	
Barley PNPi-OE Transgenic Plants	PNPi-OE-F	ggactagtATGCCGCACTACCTTGACTCAG	933
	PNPi-OE-R	ggagctcttaTTCTTTGACATGCCAGAGGATA	
Barley NPR1-OE Transgenic Plants	TaNPR1-OE-F	ggactagtATGGAGGCCCCGAGCAGCCACGTC	1719
	TaNPR1-OE-R	ggagctcttaTCTCCTAGTTCGACCTGCC	
Barley NPR1-OE Transgenic test	wNPR1-transG-F	ATCCACCTTCCAGGTCGG	543
	wNPR1-transG-R	TGGTTAAAAGGGAGACAACAATTTTA	
Amino acid substitution mutations for PNPi	PNPi-A239W-F	GGTTATAGCGGAAAAtggACTTTCTTTACTCAG	
	PNPi-A239W-R	CTGAGTAAAGAAAGTccaTTTTCCGCTATAACC	
	PNPi-T240F-F	TATAGCGGAAAAGCCtttTTCTTTACTCAGGAT	
	PNPi-T240F-R	ATCCTGAGTAAAGAAaaaGGCTTTTCCGCTATA	
	PNPi-Q244C-F	GCCACTTTCTTTACTtgtGATGGCAACGCAGGC	
	PNPi-Q244C-R	GCCTGCGTTGCCATCacaAGTAAAGAAAGTGGC	
	PNPi-G249L-F	CAGGATGGCAACGCActtGCCTGCGGCAAAACC	
	PNPi-G249L-R	GGTTTTGCCGCAGGCaagTGCGTTGCCATCCTG	
	PNPi-C251E-F	GGCAACGCAGGCGCCgaaGGCAAAACCCACCAA	
	PNPi-C251E-R	TTGGTGGGTTTTGCCttcGGCGCCTGCGTTGCC	
	PNPi-G252L-F	AACGCAGGCGCCTGCcttAAAACCCACCAAGAC	
	PNPi-G252L-R	GTCTTGGTGGGTTTTaagGCAGGCGCCTGCGTT	
	PNPi-D257W-F	GGCAAAACCCACCAAtggAGTGATTACATCGTC	
	PNPi-D257W-R	GACGATGTAATCACTccaTTGGTGGGTTTTGCC	
	PNPi-A263W-F	AGTGATTACATCGTCtggATTCAAAGTGGAATG	
	PNPi-A263W-R	CATTCCACTTTGAATccaGACGATGTAATCACT	
	PNPi-D308W-F	TCCACGTACAGTTTGtggTTATCAACGGGCGCC	
	PNPi-D308W-R	GGCGCCCGTTGATAAccaCAAACTGTACGTGGA	
	PNPi-S310Y-F	TACAGTTTGGACTTAtatACGGGCGCCTTCAAT	
	PNPi-S310Y-R	ATTGAAGGCGCCCGTataTAAGTCCAAACTGTA	
	PNPi-C275E-F	GGTGGTGGGACTTTTgaaGGCAAGACTATCGTT	
	PNPi-C275E-R	AACGATAGTCTTGCttcAAAAAGTCCCACCACC	

Supplementary Table S2. Primers used for qRT-PCR expression studies.

Primer Name	Primer Sequence 5' to 3'	Primer Efficiency	bp	GenBank Template
HvPR1b-qRT-F	CCAAGCTAGCCATCTTGCTC	85.0%	196	X74940
HvPR1b-qRT-R	TTGCAGTCGTTGATCCTCTG			
HvPR2-qRT-F	AAGATGTTGCCTCCATGTTTGCAG	96.7%	175	M62907
HvPR2-qRT-R	AAGTAGATGCGCATGCCGTTGAT			
HvPR4b-qRT-F	CTGTCGTGGCGGAGCAAGTA	100.5%	203	AK373131
HvPR4b-qRT-R	ATCCCGTTGGTGTCGATCTTG			
HvPR5-qRT-F	CAAGAGCGGTATCATCCATCC	93.1%	198	AF355456
HvPR5-qRT-R	CATGTTCAGCGCCCACGA			
HvChit-qRT-F	GGTTCCAGGCTACGGTGTAA	100.0%	163	X78671
HvChit-qRT-R	GTTCCGTTGGGTGTAGCAGT			
HvEF1a-qRT-F	TGGTGTCATCAAGCCTGGTATGGT	100.1%	86	Z50789
HvEF1a-qRT-R	ACTCATGGTGCATCTCAACGGACT			
PNPi-qRT-F	CTATTCTTCAAGCCATCAGCA	112.3%	187	KT764125
PNPi-qRT-R	CCCACCACCATACATTCCA			
PstEF-qRT-F	TTCGCCGTCCGTGATATGAGACAA	89.3%	159	GR302879
PstEF-qRT-R	ATGCGTATCATGGTGGTGGAGTGA			
NPR1-qRT-F	CCAAAACAGTCGAACTCGGCAA	94.7%	217	JX424315
NPR1-qRT-R	GACGATGAGGAAGATGAAAGGGTTG			

**Supplementary Table S3.** Transgenic lines used in qRT-PCR assays.

| Trans. Event	Genotypes	Treatment	Reps
1	WT	WATER	8
		DC3000	8
	PNPi-OE-E1-T1	WATER	8
		DC3000	8
2	WT	WATER	8
		DC3000	12
	PNPi-OE-E2-T1	WATER	12
		DC3000	16
3	WT	WATER	8
		DC3000	7
	PNPi-OE-E4-T1	WATER	8
		DC3000	7
4	WT	WATER	8
		DC3000	8
	PNPi-OE-E1-T2	WATER	3
		DC3000	3
5	WT	WATER	2
		DC3000	7
	HvNPR1-RNAi-T5	WATER	4
		DC3000	5
6	WT	WATER	5
		DC3000	11
	HvNPR1-RNAi-T5	WATER	7
		DC3000	9
7	WT	WATER	6
		DC3000	7
	TaNPR1-OE-E1-T1	WATER	8
		DC3000	8
8	WT	WATER	5
		DC3000	9
	TaNPR1-OE-E2-T1	WATER	7
		DC3000	5
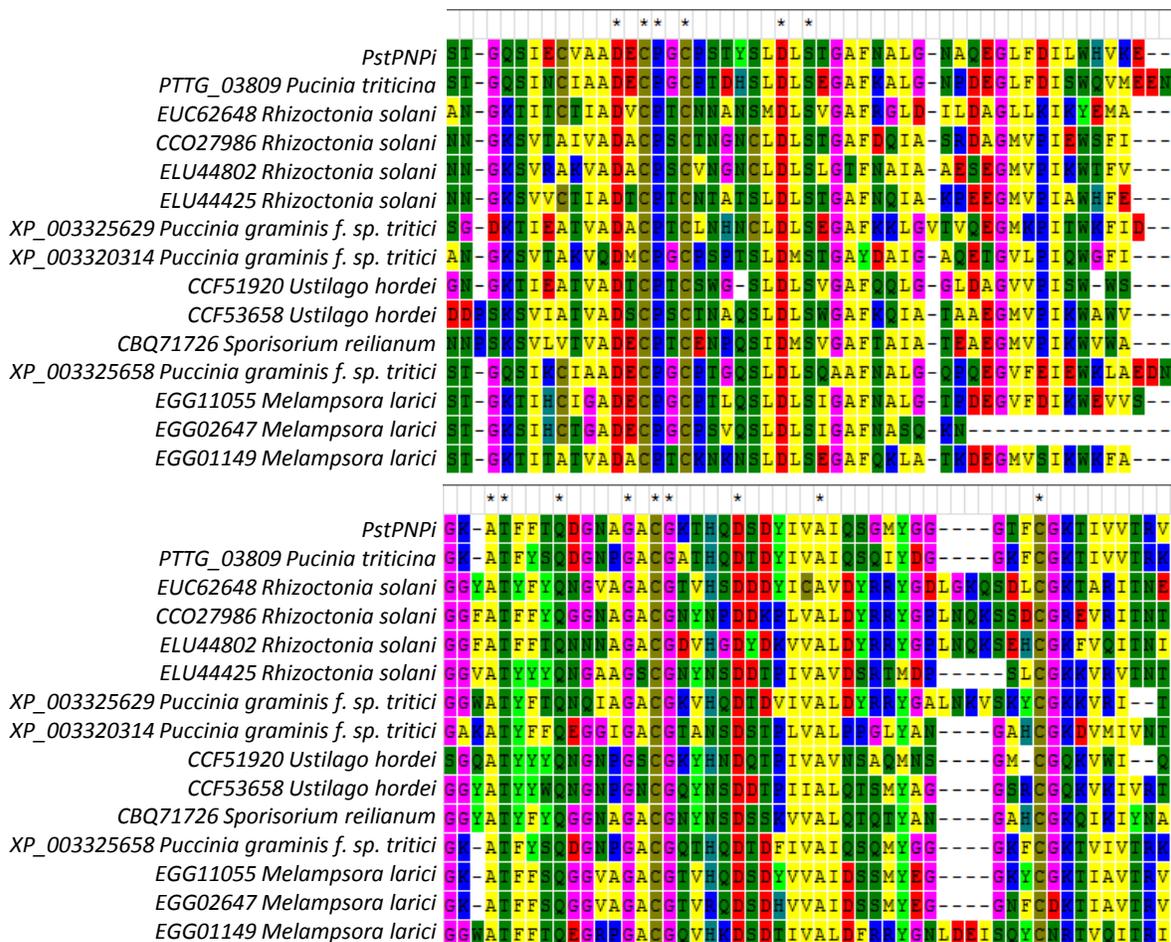
Supplementary Fig. S1. Alignments of DPBB_1 domains from PNPi homologs.
Alignment of DPBB_1 domains from PNPi and its homologs in more distantly related plant
pathogens using the multiple alignment program Muscle as implemented in MEGA 6.0.
Fifteen point mutations at the DPBB_1 domain (*) were generated to test their interactions
with wNPR1.
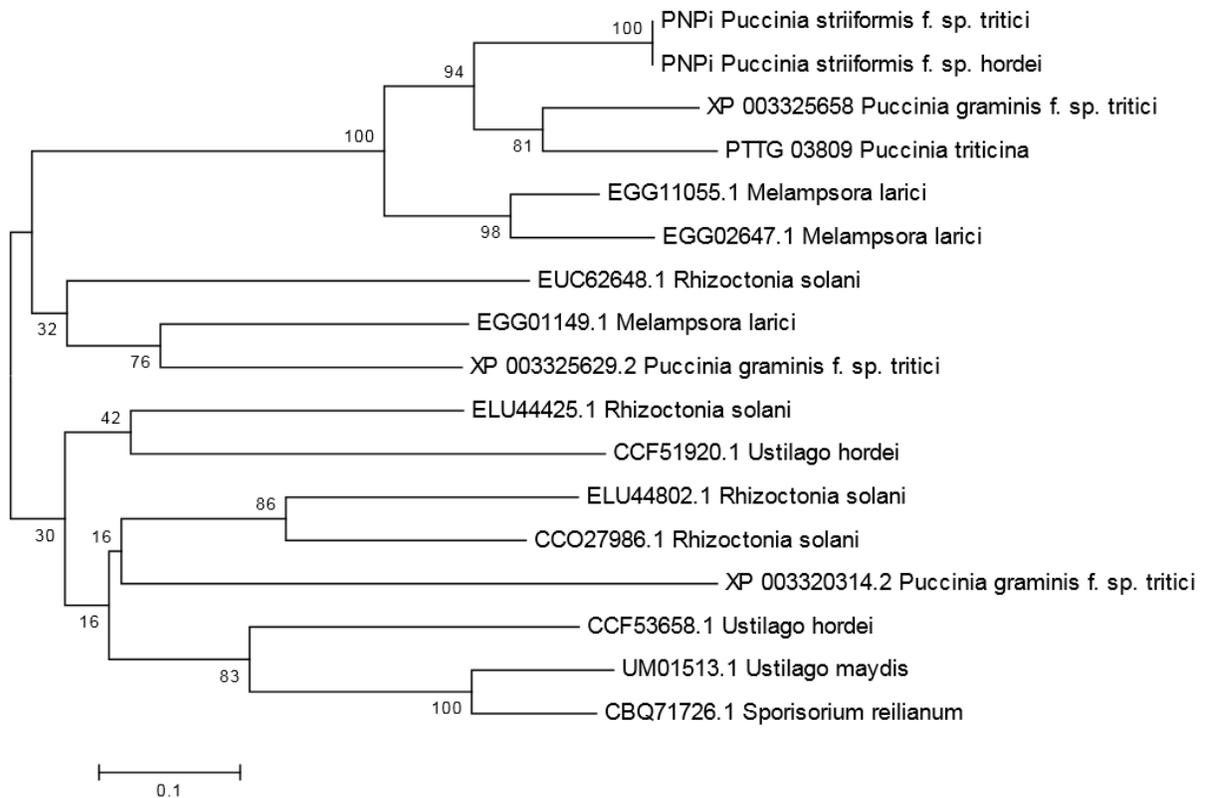
**Supplementary Fig. S2.** Neighbor-joining tree for PNPi and closest homologs from other plant pathogens. The Neighbor-joining tree was generated using the software MEGA v6. Values in the tree nodes indicate confidence values based on 1000 bootstrap replications. Alignments were based on the most conserved C-terminal region including the PPDB1 domain (last 99 amino acids of PNPi from *Puccinia striiformis* f. sp. *tritici*).
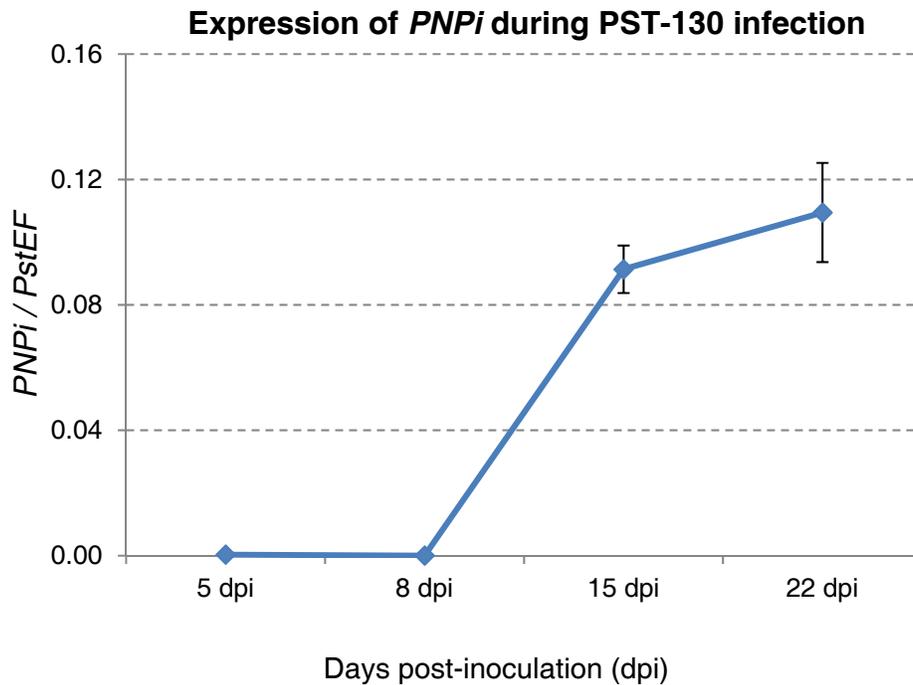
Supplementary Fig. S3. Expression of *PNPi* during PST-130 infection. Transcript levels of *PNPi* were determined by qRT-PCR in wheat leaves (cv. "Fielder") infected with *Pst* virulent race PST-130. Leaf samples were collected at 5, 8, 15, 22 days post-inoculation (dpi) with *Puccinia striiformis* f. sp. *tritici*. The Y scale indicates transcript levels of *PNPi* relative to the endogenous control *PstEF*. The mean and standard error were calculated from four independent biological replications.
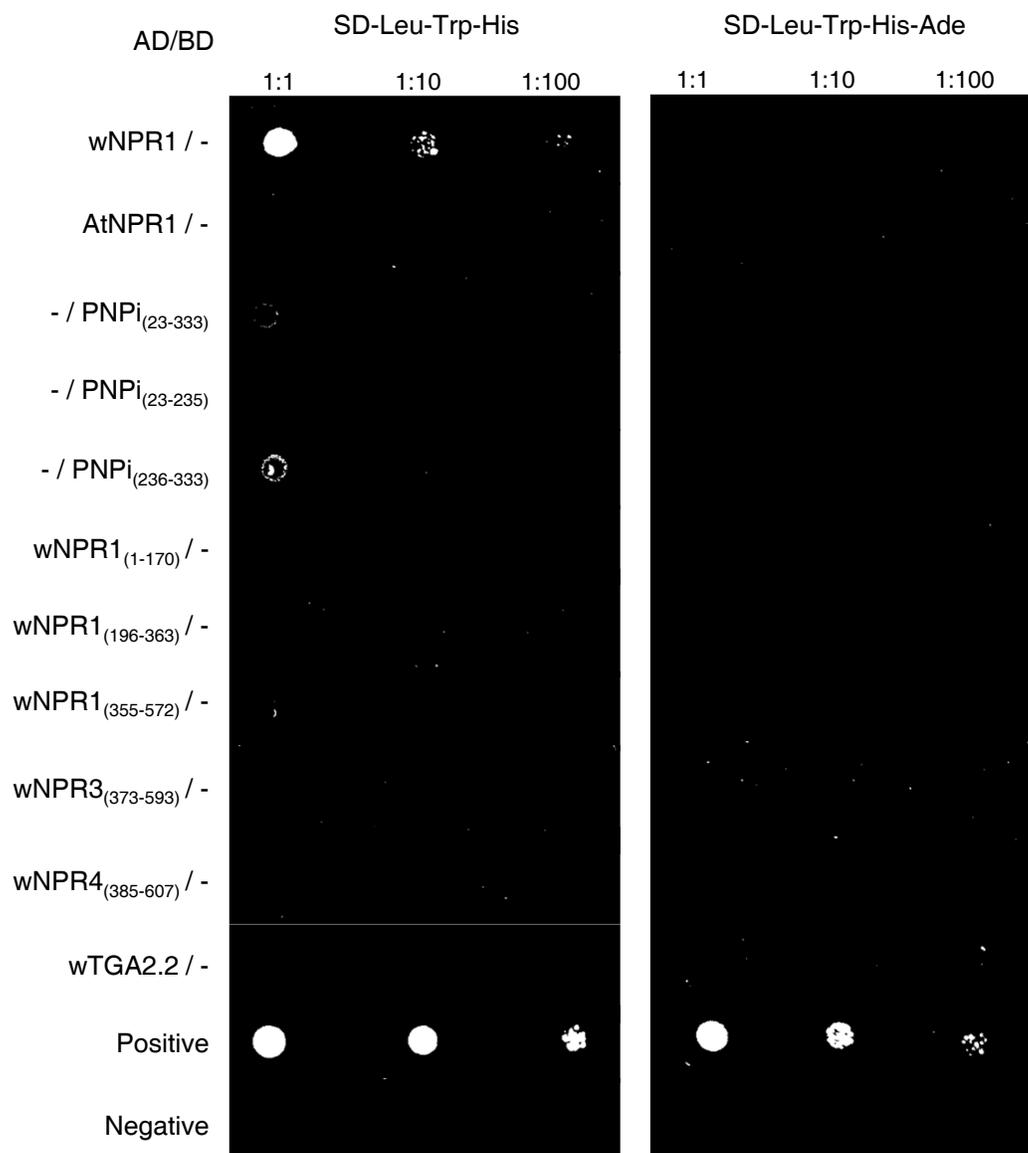
Supplementary Fig. S4. Negative controls for Y2H assay. All the bait and prey constructs were co-transformed with the corresponding empty AD or BD vectors to test auto-activation. Yeast transformants were assayed on plates with SD-Leu-Trp-His and SD-Leu-Trp-His-Ade selection media.
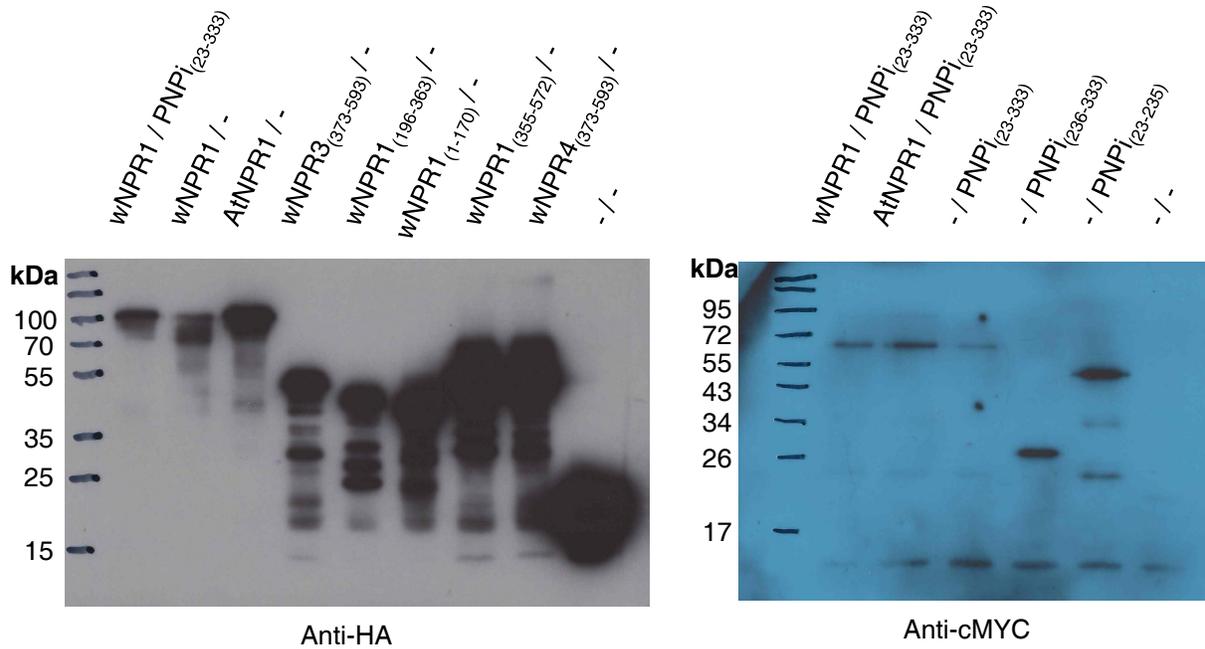
Supplementary Fig. S5. Western blot validation of protein expression in yeast two-hybrid assays with negative results. Western blot assays using anti-HA-tag and anti-cMYC-tag antibodies were applied to validate the protein expressed by either AD or BD vectors, respectively. "-" indicates empty vector.
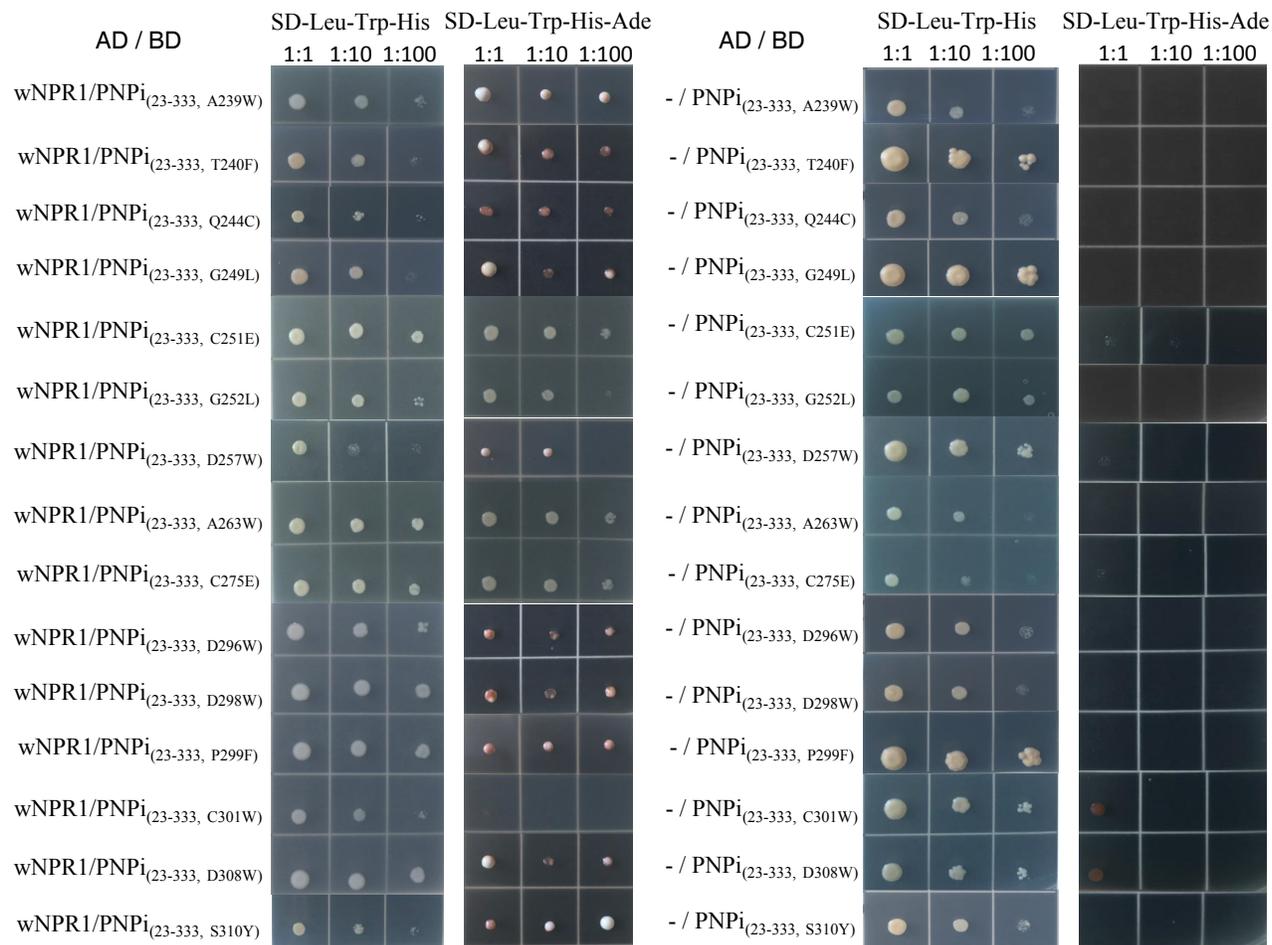
Supplementary Fig. S6. Amino acid substitutions in PNPi and their effect on the interactions with wNPR1 in yeast two-hybrid assays. Fifteen amino acid substitutions of PNPi$_{(23-333)}$ were generated by overlap-PCR and cloned into Y2H BD vectors. Yeast transformants co-expressing different bait and prey constructs were assayed on SD-Leu-Trp-His and SD-Leu-Trp-His-Ade. Point mutation C301W in PNPi was sufficient to abolish the protein interaction between these two proteins in SD-Leu-Trp-His-Ade (there is some auto-activation in SD-Leu-Trp-His).
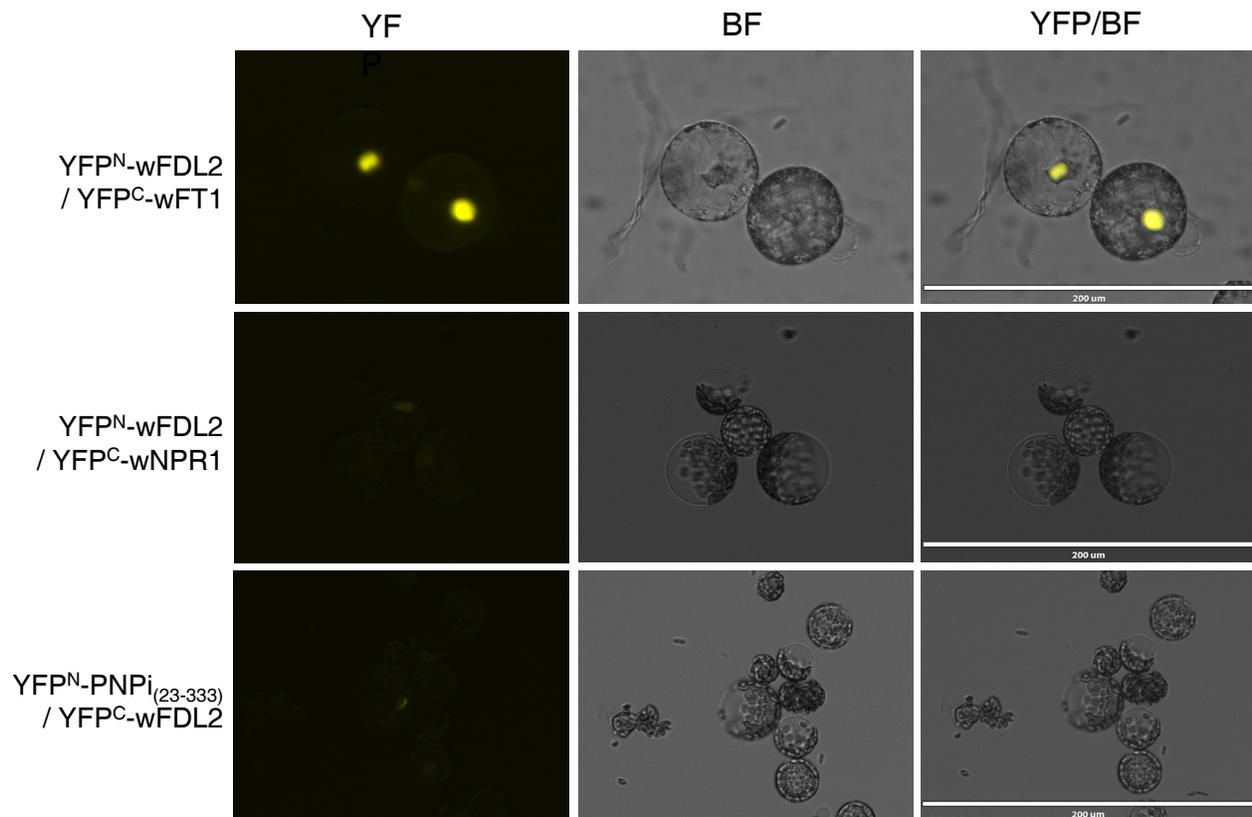
Supplementary Fig. S7. Negative controls for BiFC assays. In addition to the empty vector control, wheat protein wFDL2 was used as a nuclear localization control. Bimolecular fluorescence complementation assays showed interaction between YFP^N-wFDL2 and YFP^C-wFT in the nuclei of *N. benthamiana* protoplast. Co-expression of YFP^C-wNPR1 and YFP^N-PNPi$_{(23-333)}$ with YFP^N-wFDL2 and YFP^C-wFDL2, respectively, served as negative controls. BF = bright field; YFP = yellow fluorescent protein. Scale bars = 200 μm
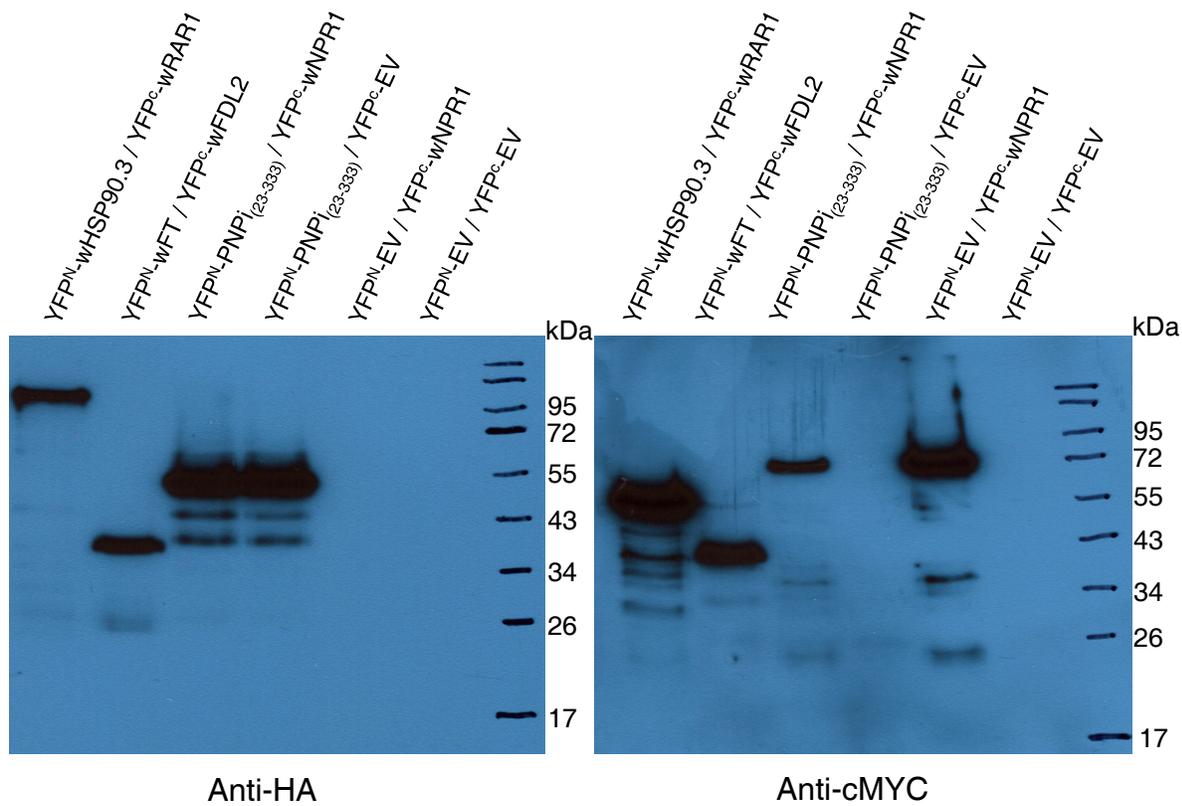
Supplementary Fig. S8. Western blot validation of protein expression in BiFC assays. Western blot assays using anti-HA-tag and anti-cMYC-tag antibodies were applied to validate the protein expressed by either pSY735 or pSY736 vectors, respectively.
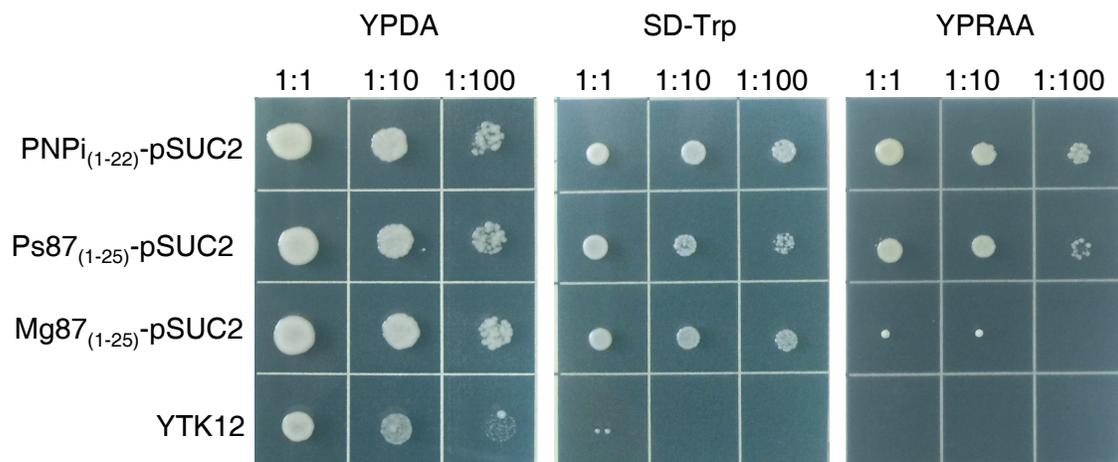
Supplementary Fig. S9. Functional validation of PNPi predicted signal peptides using a yeast invertase secretion assay. The signal peptide of PNPi was fused in frame to the invertase sequence in the pSUC2 vector and were transformed into yeast YTK12 strain. Untransformed YTK12 strain, YTK12 carrying the Ps87$_{(1-25)}$-pSUC2 (positive) and Mg87$_{(1-25)}$-pSUC2 (negative) were used as control. Strains that are unable to secrete invertase can grow on SD-Trp medium but not on YPRAA medium
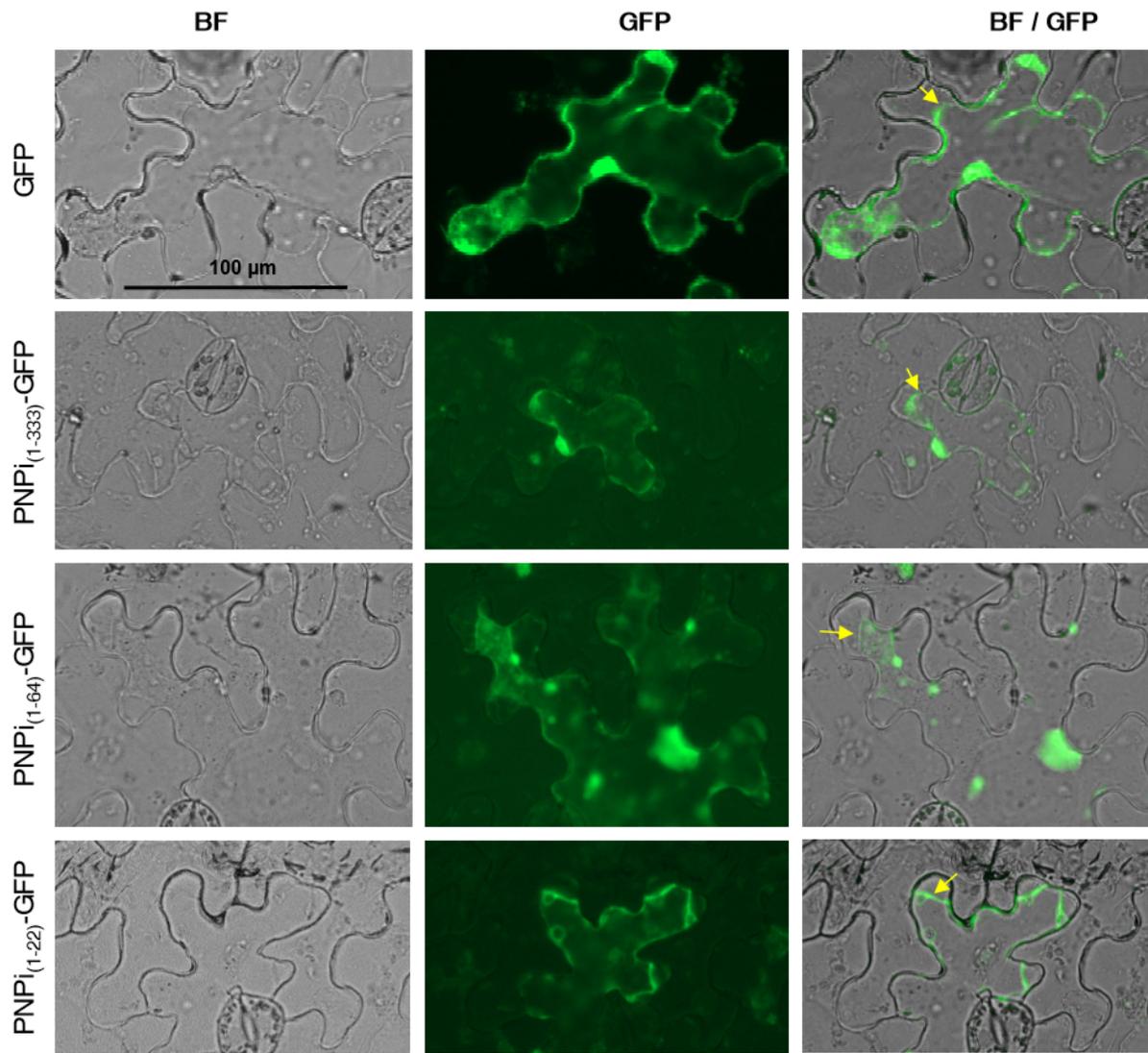
Supplementary Fig. S10. Subcellular localization of PNPi in *N. benthamiana* epidermal cells. Transient expression of GFP fused PNPi segments in *N. benthamiana* leaves by Agrobacterium infiltration. Expression in all constructs was driven by the 35S promoter. The PNPi$_{(1-22)}$-GFP fusion included only the putative signal peptide fused to GFP. The PNPi$_{(1-64)}$-GFP fusion included both the putative signal peptide and the N-terminal region including the RxLR-dEER-like motif fused to GFP. Finally, the PNPi$_{(1-333)}$-GFP fusion included the complete PNPi protein. GFP alone was used as control. Leaf epidermal peels were plasmolyzed in 800 mM mannitol for six minutes. Yellow arrows indicate examples of plasmolyzed positions, where the GFP fluorescence remains associated to the plasma membrane.

Relative expression of *Ubi::PNPi* in four transgenic events
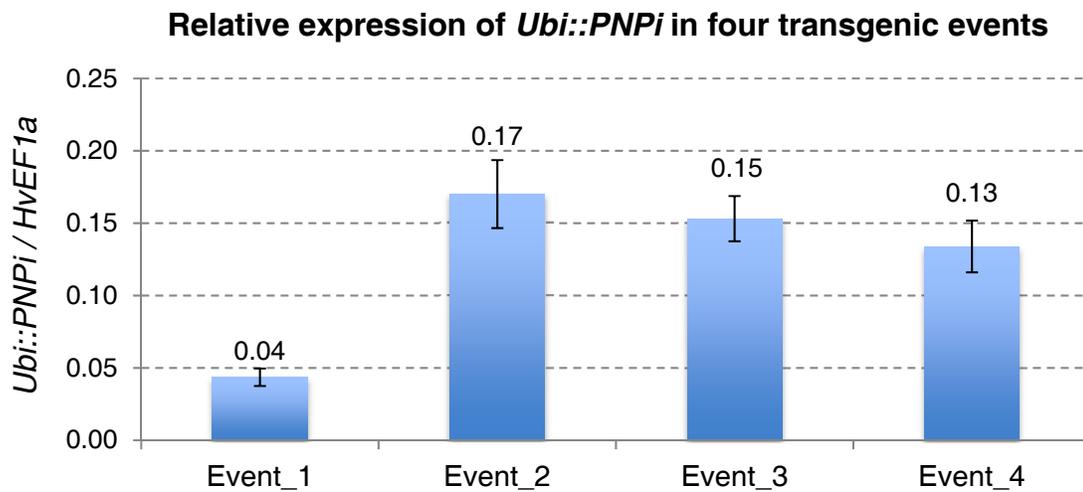
Supplementary Fig. S11. Transcript levels of *PNPi* in different *Ubi::PNPi* transgenic events in barley. Four independent barley transgenic events expressing *Ubi::PNPi* were tested. The Y scale indicates transcript levels of *PNPi* relative to the barley endogenous control *HvEF1a*. The mean and standard errors were calculated from 16 (event 1), 28 (event 2), 15 (event 3) and 6 (event 4) independent biological replicates (more information in Supplementary Table S3).
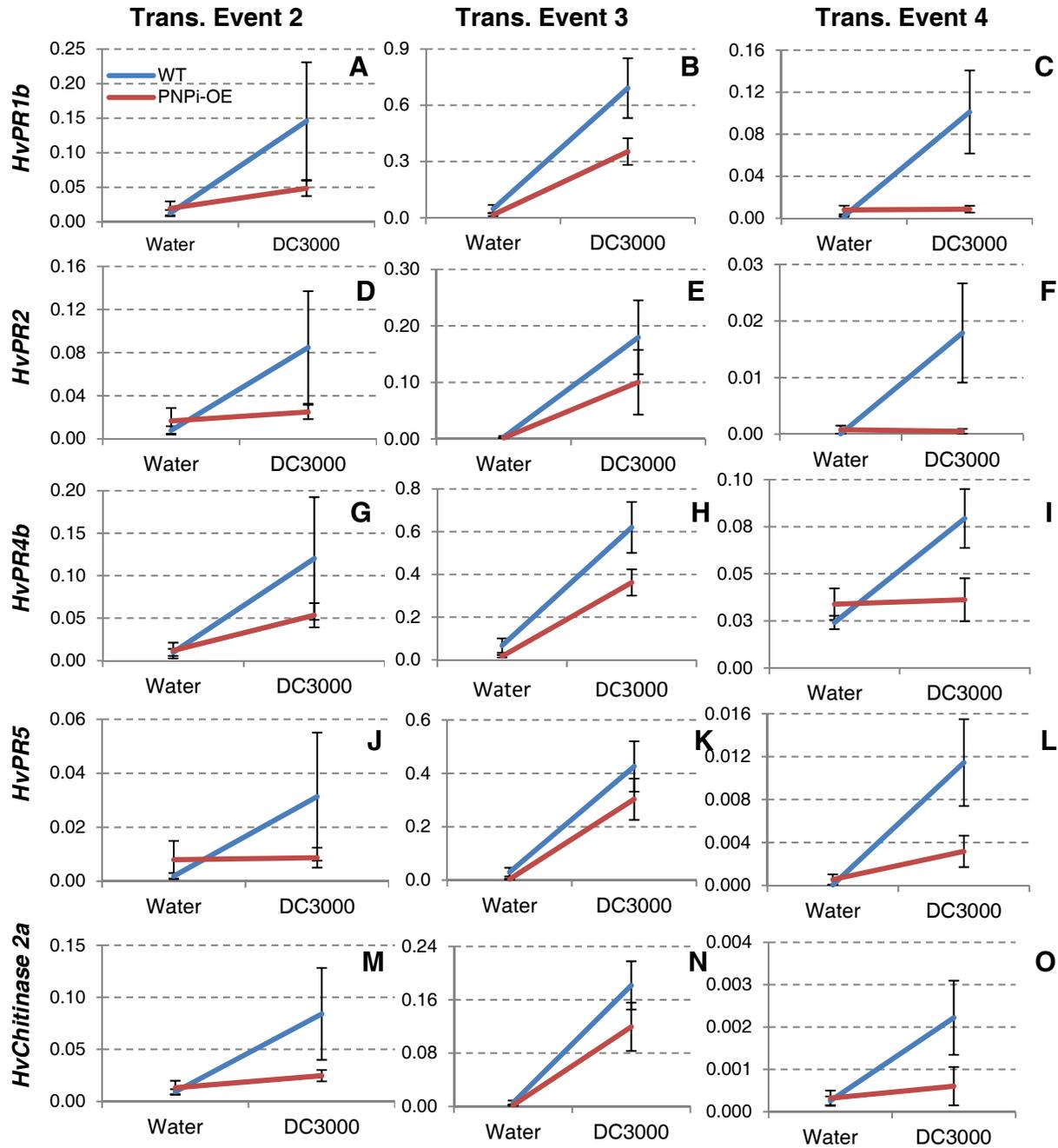
Supplementary Fig. S12. Functional characterization of transgenic barley lines overexpressing *PNPi* (*PNPi-OE*). Infiltration of young barley leaves with water (control) or *Pseudomonas syringae* pv. *tomato* DC3000. Samples for qRT-PCR assays were collected from the leaf region adjacent to the infection 48 hours after inoculation, when a weak chlorosis or yellowing occurs. Transgenic event 1 is presented in Fig. 5. Transcript levels are expressed relative to endogenous control *HvEF1a* using the $2^{-\Delta CT}$ method. Scales are not comparable between different genes or events because different optimum thresholds were used in the qRT-PCR analyses. Error bars indicate standard error of the means calculated from independent biological replicates
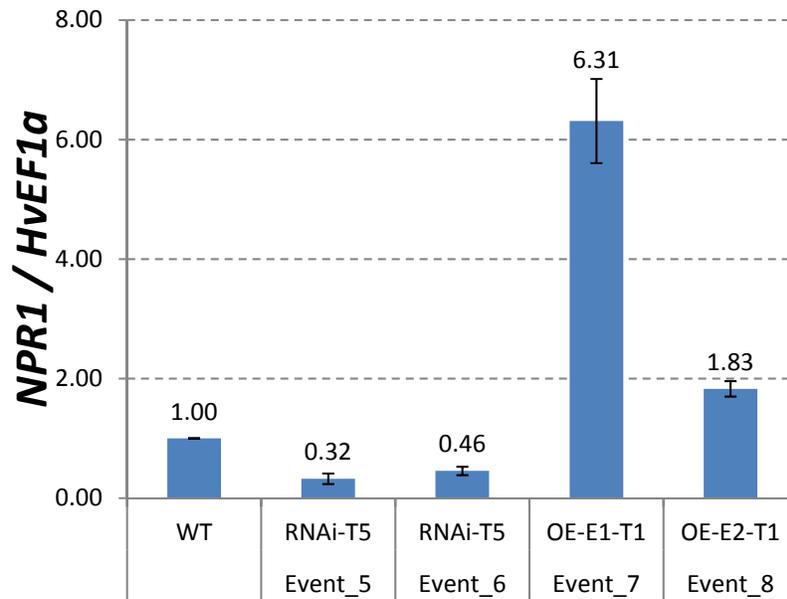
Supplementary Fig. S13. Transcript levels of *NPR1* in *Ubi::wNPR1* (overexpression) and *HvNPR1-RNAi* (downregulation) in barley transgenic plants. Expression of *NPR1* in different transgenic lines were measured by qRT-PCR. The Y scale indicates transcript levels of *NPR1* relative to the barley endogenous control *HvEF1a*. The mean and standard errors were calculated from independent biological replicates of each experiment (detail information for each transgenic event see Supplementary Table S3).
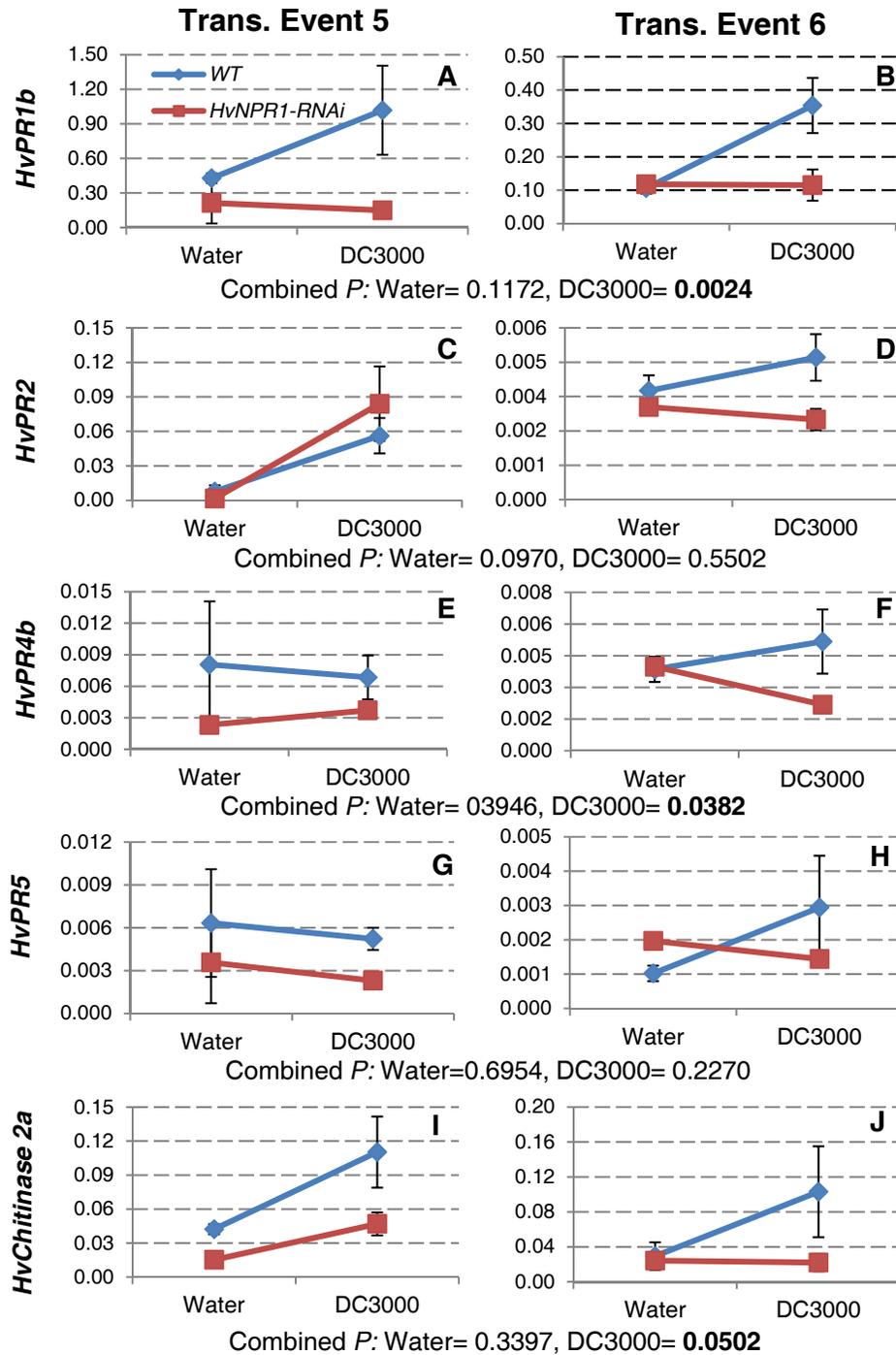
Supplementary Fig. S14. Transcript levels of *PR* genes in *HvNPR1-RNAi* transgenic barley plants. Infiltration of young barley leaves with water (control) or *P. syringae* pv. *tomato* DC3000.Samples for qRT-PCR assays were collected from the leaf region adjacent to the infection 48 h after inoculation, when a weak chlorosis or yellowing occurs. Transcript levels are expressed relative to endogenous control *EF1a* using the $2^{-\Delta CT}$ method. *P* values indicated indicate significance of the differences between transgenic and control plants in combined ANOVAs using transgenic events as blocks.

Supplementary Fig. S15. Transcript levels of *PR* genes in *Ubi::wNPR1* transgenic barley plants. Infiltration of young barley leaves with water (control) or *Pseudomonas syringae* pv. *tomato* DC3000. Samples for qRT-PCR assays were collected from the leaf region adjacent to the infection 48 hours after inoculation, when a weak chlorosis or yellowing occurs. Transcript levels are expressed relative to endogenous control *HvEF1a* using the $2^{-\Delta CT}$ method. *P* values indicate significance of the differences between transgenic and control plants in combined ANOVAs using transgenic events as blocks

```
wNPR1     1 MEAPSSHVTASFSDCDDS-VSMGDAAPD------------ADVEALRRLSDNLAAAFRSPDDFAFLADALVAVP----GA
OsNPR1    1 MEPPTSHVTNAFSDSDSASVEEGGADAD------------ADVEALRRLSDNLAAAFRSPEDFAFLADARIAVPGGGGGG
AtNPR1    1 MDTTIDGFADSYEISSTSFVATDNTDSSIVYLAAEQVLTGPDVSALQLLSNSFESVFDSPDD--FYSDAKIVLS----DG
                                                                            BTB

wNPR1    64 PDLRVHRCVLSARSPFLRALFKRRAAAAGSTGGAEGN-RLELRELL---GDEVEVGYEALELVLDYLYSGRVRDLPKSAC
OsNPR1   69 GDLLVHRCVLSARSPFLRGVFARRAAAAGGGGEDGGERLELRELLGGGGEEVEVGYEALRLVLDYLYSGRVGDLPKAAC
AtNPR1   75 REVSFHRCVLSARSSSFKSALA--AAKKEKDSNNTAAVKLELKEI----AKDYEVGFDSVVTVLAYVYSSRVRPPPKGVS
                       BTB

wNPR1   140 ACVDVDGCAHVGCHPAVSFMAQVLFAASTFQVGELASLFQRHLLDFLDNVEVDNLPLILSVANLCNKSCVKLFERCLEIV
OsNPR1  149 LCVDED-CAHVGCHPAVAFMAQVLFAASTFQVAELTNLFQRRLLDVLDKVEVDNLLLILSVANLCNKSCMKLLERCLDMV
AtNPR1  149 ECADEN-CCHVACRPAVDFMLEVLYLAFIFRIPELVILYQRHLLDVVDKVVIEDTLVILKLANICGKACMKLLDRCKEII
                      BTB

wNPR1   220 VRSNLDMITLEKALPEDVIKQIIDSRITLGLASPEDNGFPNKHVRRILKALDSDDVELVRMLLTEGQTNLDDAFALHYAV
OsNPR1  228 VRSNLDMITLEKSLPEDVIKQIIDARLSLGLISPENKGFPNKHVRRIHRALDSDDVELVRMLLTEGQTNLDDAFALHYAV
AtNPR1  228 VKSNVDMVSLEKSLPEELVKEIIDRRKELGLEVPKVK----KHVSNVHKALDSDDIELVKILLLKEDHTNLDDACALHFAV
                      DUF3420                                       ANK

wNPR1   300 EHCDSKITTELLDIALADVNLRNPRGYTVLHIAGRRRDPKIVVSLLTKGARPSDITFDGRKAVQIAKRLTKHGDYFGNTE
OsNPR1  308 EHCDSKITTELLDLALADVNHRNPRGYTVLHIAARRREPKIIVSLLTKGARPADVTFDGRKAVQISKRLTKQGDYFGVTE
AtNPR1  304 AYCNVKTATDLLKLDLADVNHRNPRGYTVLHVAAMRKEPQLILSLLEKGASASEATLEGRTALMIAKQATMAVECNNIPE
                      ANK                                           NPR1/INM1

wNPR1   380 EGKPSPNDKLCIEILEQAERRDPQLGEASVSLALAGDCLRGKLLYLENRVALARIMFPIEARVAMDIAQVDGTLEFTLGS
OsNPR1  388 EGKPSPKDRLCIEILEQAERRDPQLGEASVSLAMAGESLRGRLLYLENRVALARIMFPMEARVAMDIAQVDGTLEFNLGS
AtNPR1  384 QCKHSLKGRLCVEILEQEDKREPIPRDVPPSFAVAADELKMTLLDLENRVALAQRLFPTEAQAAMEIAEMKGTCEFIVTS
                           NPR1/INM1 C-terminal                                    ▼▼           ▼

wNPR1   460 -STNPPLEI--TTVDLNDTSFKMKEEHLARMRALSKTVELGKRFFPRCSNVLDKIMD-DEPELASLGRDASSERR----R
OsNPR1  468 -GANPPPERQRTTVDLNESPFIMKEEHLARMTALSKTVELGKRFFPRCSNVLDKIMD-DETDPVSLGRDTSAEKR----K
AtNPR1  464 LEPDRLTGTKRTSPGVKIAPFRILEEHQSRLKALSKTVELGKRFFPRCSAVLDQIMNCEDLTQLACGEDDTAEKRLQKKQ

          ▼              ▼
wNPR1   532 RFHDLQDALLKAFSEDKEEFNKTTTLSSSSSST--STVARNLTGR---PRR
OsNPR1  542 RFHDLQDVLQKAFHEDKEENDRSG-LSSSSSST--SIGAIR-------PRR
AtNPR1  544 RYMEIQETLKKAFSEDNLELGNSS-LTDSTSSTSKSTGGKRSNRKFSHRRR
              NPR1/INM1
```

Supplementary Fig. S16. Comparison of NPR1 proteins. Alignment of NPR1 and NPR1-like proteins from Arabidopsis (GenBank AAM65726.1), rice (GenBank NP_001042286.1) and wheat (GenBank AGH18701) using the multiple alignment program Muscle as implemented in MEGA 6.0. BTB = Broad-Complex, Tramtrack and Bric a brac (smart00225), DUF3420 = Domain of unknown function (pfam11900), ANK = ankyrin repeats that mediate protein-protein interactions (cd00204), NPR1/NIM1 = NPR1/NIM1-like defence protein C terminal (pfam12313).